AMPTIAC

AI-AEC-12694
COPY

BIAXIAL STRESS-RUPTURE PROPERTIES OF AUSTENITIC STAINLESS STEELS IN STATIC SODIUM

AEC Research and Development Report

ATOMICS INTERNATIONAL
A DIVISION OF NORTH AMERICAN ROCKWELL CORPORATION

Printed in the United States of America
Available from
Clearinghouse for Federal Scientific and Technical Information
National Bureau of Standards, U.S. Department of Commerce
Springfield, Virginia 22151
Price: Printed Copy $3.00; Microfiche $0.65

AI-AEC-12694
METALS, CERAMICS,
AND MATERIALS

BIAXIAL STRESS-RUPTURE PROPERTIES OF AUSTENITIC STAINLESS STEELS IN STATIC SODIUM

By
W. T. LEE

ATOMICS INTERNATIONAL
A DIVISION OF NORTH AMERICAN ROCKWELL CORPORATION

CONTRACT: AT(04-3)-701
ISSUED: JUNE 30, 1968

DISTRIBUTION

This report has been distributed according to the category "Metals, Ceramics, and Materials" as given in the Standard Distribution for Unclassified Scientific and Technical Reports, TID-4500.

ACKNOWLEDGMENT

The author wishes to acknowledge the vital contribution of M. G. Metcalf and L. V. Custer in preparing and conducting the stress-rupture tests. Many thanks are due to D. F. Atkins for his guidance and suggestions. Appreciation is also extended to D. Kramer and J. H. Shively for their discussions.

CONTENTS

TABLES

FIGURES

FIGURES

ABSTRACT

The mechanical properties of candidate cladding materials for fast breeder reactor fuel elements are being investigated as part of the Atomic Energy Commission Liquid Metal Cooled Fast Breeder Reactor Program. This report deals with the stress-rupture characteristics of austenitic stainless steels in a liquid sodium environment, in both cold-worked and annealed conditions.

Results of the following biaxial (2:1) stress-rupture tests in high-purity ($O_2 \sim 10$ ppm) sodium are presented:

1) 10 to 15% cold-worked Type 304 stainless steel tested at 1000, 1100, 1200, and 1400° F for periods up to 4000 hr

2) Annealed Type 304 stainless steel tested at 1200 and 1400° F for periods up to 2000 hr

3) 10 to 15% cold-worked Type 316 stainless steel tested at 1000, 1200, and 1400° F for periods up to 4000 hr

4) Annealed Type 316 stainless steel tested at 1200 and 1400° F for periods up to 3000 hr.

For both austenitic stainless steels, the short-term rupture strength, rupture life, and diametral strain of thin-walled tubing in an environment of high-purity sodium were unchanged from results obtained when tested in an atmosphere of high-purity helium. High-purity liquid sodium exhibits the same lack of effect on 10 to 15% cold-worked and annealed austenitic stainless steels. Cold-worked austenitic stainless steel tubing, in comparison with annealed material, was found to have lower long-term rupture strength, when tested at temperatures where recovery processes are operative. Cold work also reduced diametral strain. The formation of sigma phase was detected, and is attributed largely to cold work and creep deformation.

In comparison with the rupture strength of 10 to 15% cold-worked Type 304 stainless steel tested at 1400 and 1200° F, 10 to 15% cold-worked Type 316 stainless steel was found to possess significantly higher long-term rupture strength and comparable ductility (diametral strain).

72885 Wong

July 15, 1968

ERRATA
TO
BIAXIAL STRESS-RUPTURE PROPERTIES
OF
AUSTENITIC STAINLESS STEELS
IN
STATIC SODIUM
AI-AEC-12694

The attached figure should be substituted for Figure 18, page 42.

ATOMICS INTERNATIONAL
A Division of North American Rockwell Corp.

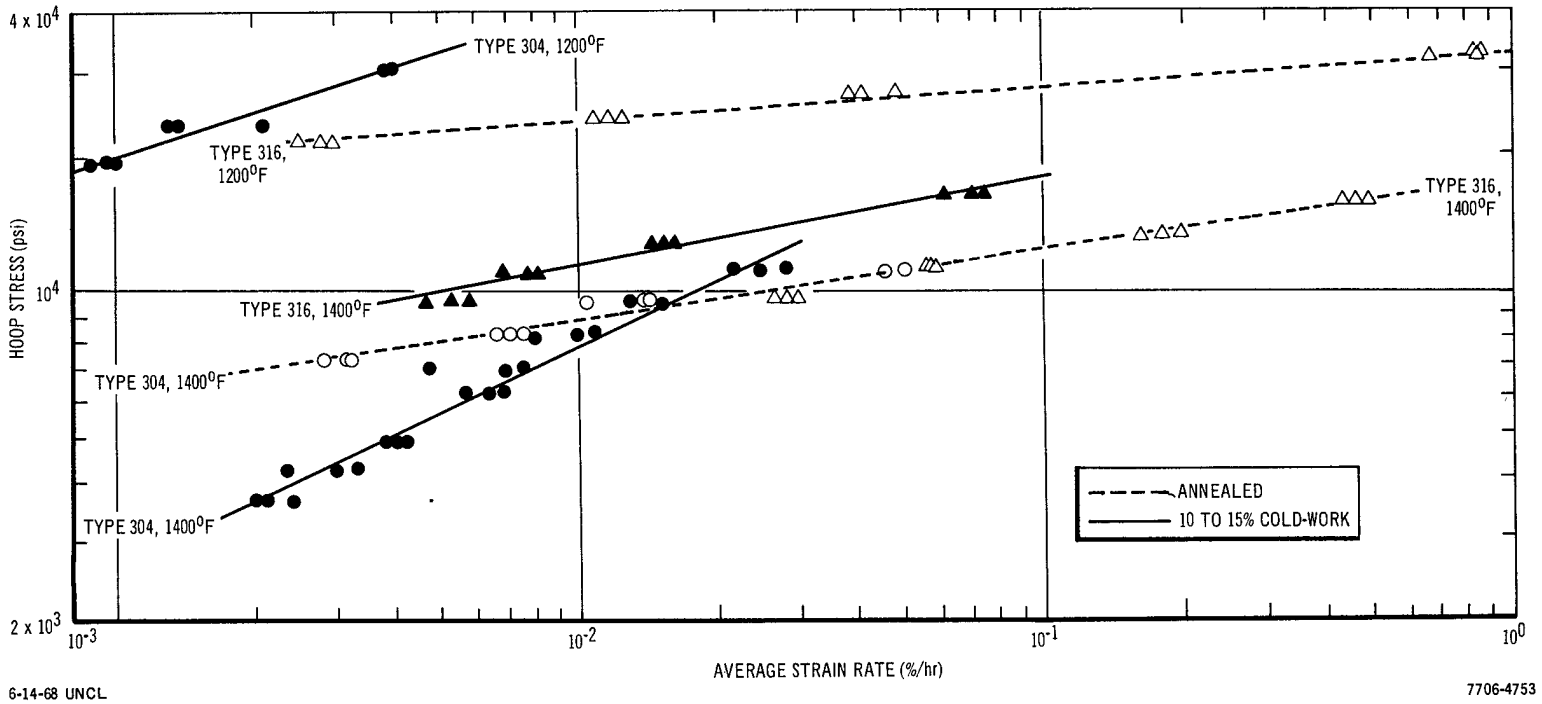

Figure 18. Variation of Strain Rate With Stress for Types 304 and 316 Stainless Steels in 1200 and 1400°F Sodium

I. INTRODUCTION

Cladding materials for use in Liquid Metal Cooled Fast Breeder Reactor (LMFBR) fuel elements will be subjected to stringent service environments, which include elevated temperatures, mechanical and thermal stresses, high heat flux with high thermal gradient across the cladding wall, high fast neutron irradiation, and liquid metal coolant. ~~This report~~ It encompasses an investigation intended to explore the effects of mechanical stress, elevated temperatures (1000 to 1400°F), and liquid sodium environment on the biaxial stress-rupture behavior of AISI Type 304 SS and Type 316 SS stainless steels.

The fact that the operating environment can affect the mechanical properties of material is both rational and well documented. The major interaction between a solid metal and its liquid metal environment is usually one of the following:

1) Brittle and premature fracture of the solid metal when under applied or residual stress, associated with intercrystalline penetration by the liquid metal[1]

2) Intercrystalline penetration by the liquid metal in the absence of stress[2]

3) Dissolution of solid metal elements into the liquid metal[3,5]

4) Solid diffusion of the liquid metal into the solid and the subsequent formation of single or multiple layers of intermetallic compounds at the original liquid-solid interface[4]

5) No apparent interaction.[6]

Tubes containing fissile fuel for the LMFBR will probably be subjected to a biaxial state of stress, due to fuel swelling and fission gas generation. Although uniaxial creep-rupture data on austenitic stainless steel in 1200°F sodium are currently available,[6] pertinent biaxial stress-rupture data in high-purity sodium are scarce or nonexistent in the literature. It is generally accepted, however, that the state of stress has pronounced effects on the mechanical properties of a material. Therefore, biaxial (2:1) tests were run to determine the effects of static liquid sodium environment on the properties of austenitic stainless steels.

Cold-worked tubing will not deform as easily as the fully annealed tubing, and it might be advantageous to incorporate some cold work in the cladding tubing to be used in a reactor, to facilitate handling and to minimize tubing surface deformation. Rostoker et al.[7] have reported that cold-worked steel, when tested in a liquid tin environment, exhibited severe degradation of mechanical properties, as compared to the mechanical properties when tested in its annealed condition. Therefore, stress-rupture tests of 10 to 15% cold-worked tubing were performed, to parallel the annealed tubing tests, in order to determine the effect of cold work on the properties in a high-temperature static liquid sodium environment.

The initial phase of studies to determine the properties of austenitic stainless steels in high-temperature liquid sodium environments (900 to 1400°F) has been completed. Data were obtained from biaxially (2:1) stressed tests on 10 to 15% cold-worked Types 304 and 316 stainless steel tubing (at 1000, 1200, and 1400°F). Scoping test data on annealed Types 304 and 316 stainless steel were obtained to determine the effect of 10 to 15% cold work on stress rupture properties at 1200 and 1400°F. Data in 1200 and 1400°F high-purity helium for 10 to 15% cold-worked austenitic stainless steels were also derived for comparison purposes.

→ p. 11

II. EXPERIMENTAL

A. MATERIALS AND EQUIPMENT

1. Test Materials

AISI Type 304 stainless steel seamless tubing of nominal 0.295-in. OD by 0.010-in. wall was used. Processing history of the material included hot finished extrusion to 7/8-in. OD by 0.083-in. nominal wall, followed by tube reduction. A normal cycle of degreasing, annealing, pickling, and cold drawing was employed to obtain the final product. In its finished form, the tubing contained 10 to 15% cold work. The average grain size of the tubing was ASTM 8.[8]

The annealed Type 304 stainless steel tubing was obtained by annealing sections (24 in. in length) of the as-received Type 304 stainless steel (10 to 15% cold work) tubing for 30 min at 1900° F in dry hydrogen. The average grain size of the annealed tubing was ASTM 7.

AISI Type 316 stainless steel tubing of nominal 0.295-in. OD by 0.010-in. wall was subjected to a process history identical to that described for Type 304 stainless steel. In its finished form, the tubing contained 10 to 15% cold work. The average grain size of the as-received tubing was ASTM 7.

The annealed Type 316 stainless steel tubing was obtained by annealing sections (24 in. in length) of the 10 to 15% cold-worked Type 316 stainless steel tubing for 30 min at 1950° F in dry hydrogen. The average grain size of the annealed tubing was ASTM 6.

Chemical compositions and short-term tensile properties of the materials used are shown in Table 1. After eddy-current inspection for subsurface defects, the tubing was cut into specimens, 4 in. long. The tubular specimens were joined to end plugs and pressurizing tubes by electron-beam welding in a 10^{-4} torr vacuum. The outside diameter of each specimen was measured to ±0.0001 in. with a profilometer. The wall thickness was measured to ±0.0001 in. with a Vidigage. The wall thickness variation in a specimen was usually low (within ±0.0005 in.)

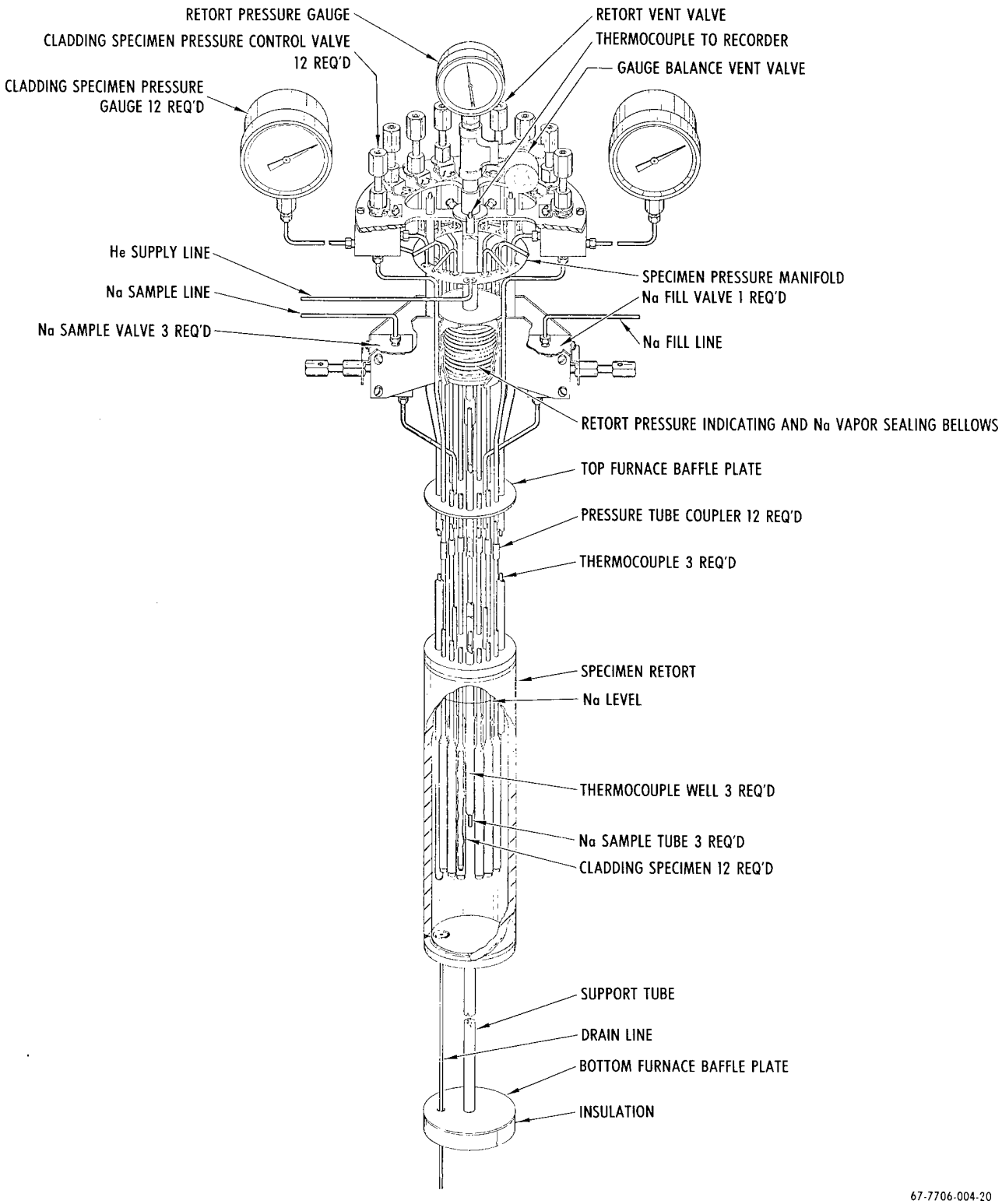

Figure 1. Twelve-Specimen Static Sodium Assembly for Biaxial Cladding Tests

TABLE 1

CHARACTERIZATION OF AS-RECEIVED (10 to 15% Cold-Worked) TYPES 304 AND 316 STAINLESS STEEL

Properties	Type 304 Stainless Steel (Heat No. 20013)	Type 316 Stainless Steel (Heat No. 65808)
Chemistry:		
Element	(wt %)	(wt %)
Cr	18.66	17.43
Ni	9.30	13.4
Mn	1.50	1.83
Si	0.30	0.45
Mo	0.22	2.5
Cu	0.20	0.09
C	0.06	0.012
P	<0.03	0.004
S	<0.03	0.002
Co	<0.10	0.04
B	5 ppm	<5 ppm
N_2	750 ppm	700 ppm
Room Temperature Tensile Properties		
0.2% Yield Strength (psi)	89,000	89,000
Ultimate Strength (psi)	118,000	108,000
Elongation (2-in. gage) (%)	29	35
Hardness (R_c)	23	23

2. Sodium Retort and Assembly

The test assembly has the capability of simultaneously testing 12 tubular samples in sodium (Figure 1). The retort body was made of either Type 304 or Type 316 stainless steel, matching the material of the specimens to be tested. It was fabricated from standard Schedule 40 pipe of 2.469-in. ID and 12.5-in. length. Provisions were made for individual specimen pressurization and read-out, sodium sampling during test, and thermocouple checkout during operation.

Detailed design and assembly of the retort have been reported previously.[3] During all steps of sample preparation and retort assembly, all components were kept clean to avoid subsequent contamination of the sodium environment. Extensive helium leak checking was utilized to insure an airtight retort system.

3. Furnace System and Temperature Control

Resistance-wound tube furnaces, 3-in. ID by 24-in. long, with controllers and power transformers, were used to provide and maintain the desired test temperature. The temperature was measured at three positions along the specimen length by calibrated Chromel-Alumel thermocouples in thermocouple wells. A second calibrated set of thermocouples was used periodically to check the drift of the test thermocouples. Temperature variation of the specimens from the indicated nominal test temperature was normally within ±3°F, although occasionally it fluctuated within a ±5°F range during the test. The temperature variation along the length of the test specimen did not exceed ±2°F.

4. Test Environments

Sodium for the retort tests was supplied from a sodium supply loop, built especially to provide "system quality" sodium for the LMFBR Cladding Program. Chemical composition of the "system quality" grade sodium, and detailed procedures for sodium transfer from the supply loop to the retort, were described in an earlier report.[3] The retort was filled with ~450 cc of sodium, a quantity sufficient to allow withdrawal of several sodium samples during testing and still keep the specimens completely immersed. Helium (99.99% pure) for the tests was supplied from special high-purity helium bottles. Its chemistry, and the procedures for helium transfer, were given in the referenced report.[3]

B. TESTING

After assembly, loading with sodium, and connecting to the helium pressure lines, the retorts were brought to the desired test temperature. The samples were thereafter pressurized with high-purity helium gas to the desired stress levels (to ±0.5%). For thin-walled tubing, the required helium gas pressure (in psig) was calculated from the equation[9]

$$P = \left(\frac{2t}{D}\right)\sigma \quad , \qquad \ldots(1)$$

where

σ = intended hoop stress (psi)

D = mean diameter of the tubing (in.)

t = average minimum wall thickness (in.).

The load was applied gradually, to avoid shock or overloading. The pressure gauges were monitored on a semi-daily basis. A failed specimen was identified by a pressure loss on the specimen gauge and a concurrent rise of retort gauge pressure.

Three sodium samples were extracted from the static sodium retort during each test for chemical analysis. The first sample was taken at the beginning of the stress-rupture test; the second, at the estimated middle of the test; the final sampling occurred when all the tubing specimens had ruptured. Detailed sampling procedures were described in a previous report.[3]

C. POST-TEST MEASUREMENTS AND EXAMINATIONS

After all the specimens had ruptured and the last sodium sample was obtained and analyzed, the retort was drained of sodium, dismantled, and the specimens soaked in a bath of pure isopropyl alcohol to remove sodium from the tubing surfaces. The diameter of the cleaned specimens was measured by a profilometer to ±0.0001 in. The rupture regions on the specimen walls were generally small; but, in some cases, large explosive-type ruptures with localized deformation occurred. Selected specimens were sectioned for post mortem metallographic examination, hardness testing, x-ray diffraction, and chemical analysis.

III. RESULTS

The biaxial stress-rupture test matrix of Types 304 and 316 stainless steel is shown in Table 2. After testing, all tubular specimens exhibited clean surfaces and had a bright metallic appearance. Macroscopic observations showed a minute fissure-type rupture on all specimens tested at 1400°F. Both minute fissures and large explosive-type rupture openings were observed on specimens tested at 1200°F and lower. Microscopic examinations revealed that all the ruptures were intergranular. In general, Type 316 stainless steel specimens exhibited higher diametral strain than did the Type 304 stainless steel under the same test conditions. This was more pronounced with annealed tubing than with cold-worked tubing.

TABLE 2

BIAXIAL STRESS-RUPTURE TEST MATRIX OF TYPES 304 AND 316 STAINLESS STEEL

Test	Type 304 Stainless Steel						Type 316 Stainless Steel					
	Temperature (°F)						Temperature (°F)					
	900	1000	1100	1200	1300	1400	900	1000	1100	1200	1300	1400
Reference Condition*												
Scoping Tests (100 to 1000 hr)		●	●	●		●		●		●		●
Design Tests (100 to 5000 hr)	⊗	⊗		⊗		●	×					
Design Tests (to 10,000 hr)		⊗		⊗				⊗		⊗		
Variable Tests												
Annealed (100 to 5000 hr)		⊗		⊗		●	×	⊗		⊗		●
Annealed (to 10,000 hr)		⊗		⊗				⊗		⊗		
Thermal Aging (100 to 1000 hr)				⊗								
Helium† (500 to 5000 hr)				⊗		●		⊗				●
Pre-Exposed (100 to 5000 hr)				×								

*External environment – high-purity sodium, internal environment – high-purity helium.
†Both external and internal environments are helium.

Symbols: ● Test completed
⊗ Test in progress
× Test planned.

Each test contains 12 specimens.

A. AISI TYPE 304 STAINLESS STEEL IN LOW-OXYGEN (~10 ppm) SODIUM

The results of 10 to 15% cold-worked and annealed Type 304 stainless steel (Heat No. 20013), stress-rupture tested in 1200 and 1400°F sodium, are summarized in Table 3 and Figure 2. Two additional retorts, each containing 12 cold-worked specimens from the same heat, were tested in 1200 and 1400°F high-purity helium environment. As is also shown in Table 3 and Figure 2, the data for two retorts, each containing twelve 10 to 15% cold-worked Type 304 stainless steel samples, tested in 1000 and 1100°F sodium, were included.

Compared with the tests of annealed Type 304 stainless steel in 1200 and 1400°F sodium, the long-term rupture life of cold-worked Type 304 stainless steel is reduced. When compared to the same heat of 10 to 15% cold-worked Type 304 stainless steel tested in high-purity helium, sodium appeared to have no effect on the stress-rupture strength of Type 304 stainless steel, up to a testing time of about 4000 and 1000 hr at 1200 and 1400°F, respectively (Figure 3).

Metallographic examination of transverse and longitudinal sections of the as-received tubing revealed normal structures.[3] Microstructural observations of the cold-worked samples tested in 1400°F sodium revealed intergranular fracture with an extensive amount of "r"-type (rounded-type) grain boundary voids (Figure 4).[5] Carbides were found on grain boundaries, on twin boundaries, and on slip bands in the grain matrix. Sigma particles, revealed by selective etching, were randomly distributed on grain boundaries, with heavier concentration at the ID and OD of the tubing (where prior cold work was heavier). No reaction layer was observed on the OD of tubing in contact with liquid sodium. X-ray diffraction on the OD of tubing tested for 813 hr revealed only austenite. Compared to the microstructure of the material tested for 813 hr (Figure 4a), the size and amount of sigma particles in the specimen tested for 3032 hr (Figure 4b) was greater, indicating that sigma formation increased with time at 1400°F. The hardness of ruptured tubing was reduced by 3000 hr of testing at 1400°F (from R_c23 to R_b93).

Microscopic examination of the ruptured annealed specimens revealed similar intergranular failures, with a very small amount of "w"-type (wedge-type) voids along the grain boundaries close to the rupture. Carbide precipitation was observed on grain boundaries, and a small amount was also found within

TABLE 3 (Sheet 1 of 2)

BIAXIAL STRESS-RUPTURE DATA FOR TYPE 304 STAINLESS STEEL
(Heat No. 20013)

Alloy Condition	Environment	Temperature (°F)	Specimen Number	Hoop Stress (psi)	Rupture Time (hr)	Diametral Strain (maximum) (%)
10 to 15% Cold Work (As-received)	Sodium ($O_2 \sim 10$ ppm)	1400	4-64	11,000	201	5.6
			-63	11,000	201	4.9
			-62	11,000	222	4.7
			-61	9,500	320	5.2
			-60	9,500	332	4.9
			-59	9,500	296	3.8
			-58	8,000	512	5.0
			-57	8,000	512	5.5
			-56	8,000	455	3.5
			-55	6,800	813	6.1
			-54	6,800	682	3.2
			-53	6,800	775	5.3
			4-100	6,000	825	5.7
			-99	6,000	696	3.8
			-98	6,000	849	5.4
			-97	4,700	1402	5.4
			-96	4,700	1449	6.0
			-95	4,700	1488	5.9
			-94	4,100	1785	4.2
			-93	4,100	1990	6.7
			-92	4,100	2192	6.4
			-91	3,500	3032	7.3
			-90	3,500	2864	5.7
			-89	3,500	2915	5.8
Annealed	Sodium ($O_2 \sim 10$ ppm)	1400	A4-139	11,000	230	13.8
			-138	11,000	230	10.5
			-137	11,000	250	12.5
			-136	9,500	552	11.1
			-135	9,500	468	11.3
			-134	9,500	502	12.0
			-133	8,000	1260	8.7
			-132	8,000	1306	7.4
			-131	8,000	1094	8.2
			-130	7,200	2120	5.8
			-129	7,200	1834	5.8
			-128	7,200	2073	6.7
10 to 15% Cold Work (As-received)	Sodium ($O_2 \sim 10$ ppm)	1200	4-112	35,000	273	Burst
			-111	35,000	297	Burst
			-110	35,000	297	Burst
			-109	30,000	765	3.0
			-108	30,000	743	Burst
			-107	30,000	729	2.8
			-106	23,000	1305	2.7
			-105	23,000	2030	2.6
			-104	23,000	2030	2.7
			-103	19,000	3400	3.3
			-102	19,000	3273	3.3
			-101	19,000	3360	3.0

TABLE 3 (Sheet 2 of 2)

BIAXIAL STRESS-RUPTURE DATA FOR TYPE 304 STAINLESS STEEL

(Heat No. 20013)

Alloy Condition	Environment	Temperature (°F)	Specimen Number	Hoop Stress (psi)	Rupture Time (hr)	Diametral Strain (maximum) (%)
Annealed	Sodium ($O_2 \sim 10$ ppm)	1200	A4-24	35,000	58	In Progress
			-23	35,000	58	
			-22	35,000	37	
			-21	30,000	228	
			-20	30,000	228	
			-19	30,000	228	
			-17	25,000	850	
			-16	25,000	875	
			-15	19,000	In Progress	
			-14	19,000	In Progress	
			-13	19,000	In Progress	
10 to 15% Cold Work	Sodium ($O_2 \sim 10$ ppm)	1100	4-76	43,000	737	1.9
			-75	43,000	675	Burst
			-74	43,000	494	Burst
			-73	40,000	1328	Burst
			-72	40,000	1174	Burst
			-71	40,000	1125	Burst
			-70	38,000	1477	1.5
			-69	38,000	1560	Burst
			-68	38,000	1760	1.5
			-67	35,000	3300	1.9
			-66	35,000	3373	1.7
			-65	35,000	3206	1.5
10 to 15% Cold Work	Helium (99.99%)	1400	4-36	9,950	263	6.0
			-35	9,950	267	5.1
			-34	9,950	263	5.1
			-33	8,570	344	6.1
			-32	8,570	344	3.4
			-31	8,570	380	4.8
			-30	7,200	531	4.0
			-29	7,200	503	4.7
			-28	7,200	584	5.7
			-27	6,140	789	7.1
			-26	6,140	710	5.1
			-25	6,140	734	5.8
10 to 15% Cold Work	Helium (99.99%)	1200	4-148	35,000	372	In Progress
			-147	35,000	372	In Progress
			-146	35,000	Discontinued	-
			-151	28,000	1257	In Progress
			-150	28,000	1233	In Progress
			-149	28,000	Discontinued	-
			4-145	22,000	2751	In Progress
			-144	22,000	2783	In Progress
			-143	22,000	2937	In Progress
			-142	17,000	In Progress	In Progress
			-141	17,000	In Progress	In Progress
			-140	17,000	In Progress	In Progress
10 to 15% Cold Work	Sodium ($O_2 \sim 10$ ppm)	1000	4-88	75,000	58	Burst
			-87	75,000	45	Burst
			-86	75,000	58	Burst
			-85	70,000	105	Burst
			-84	70,000	155	Burst
			-83	70,000	179	Burst
			-82	65,000	285	Burst
			-81	65,000	321	Burst
			-80	65,000	225	Burst
			-79	60,000	550	Burst
			-78	60,000	Discontinued	-
			-77	60,000	680	Burst

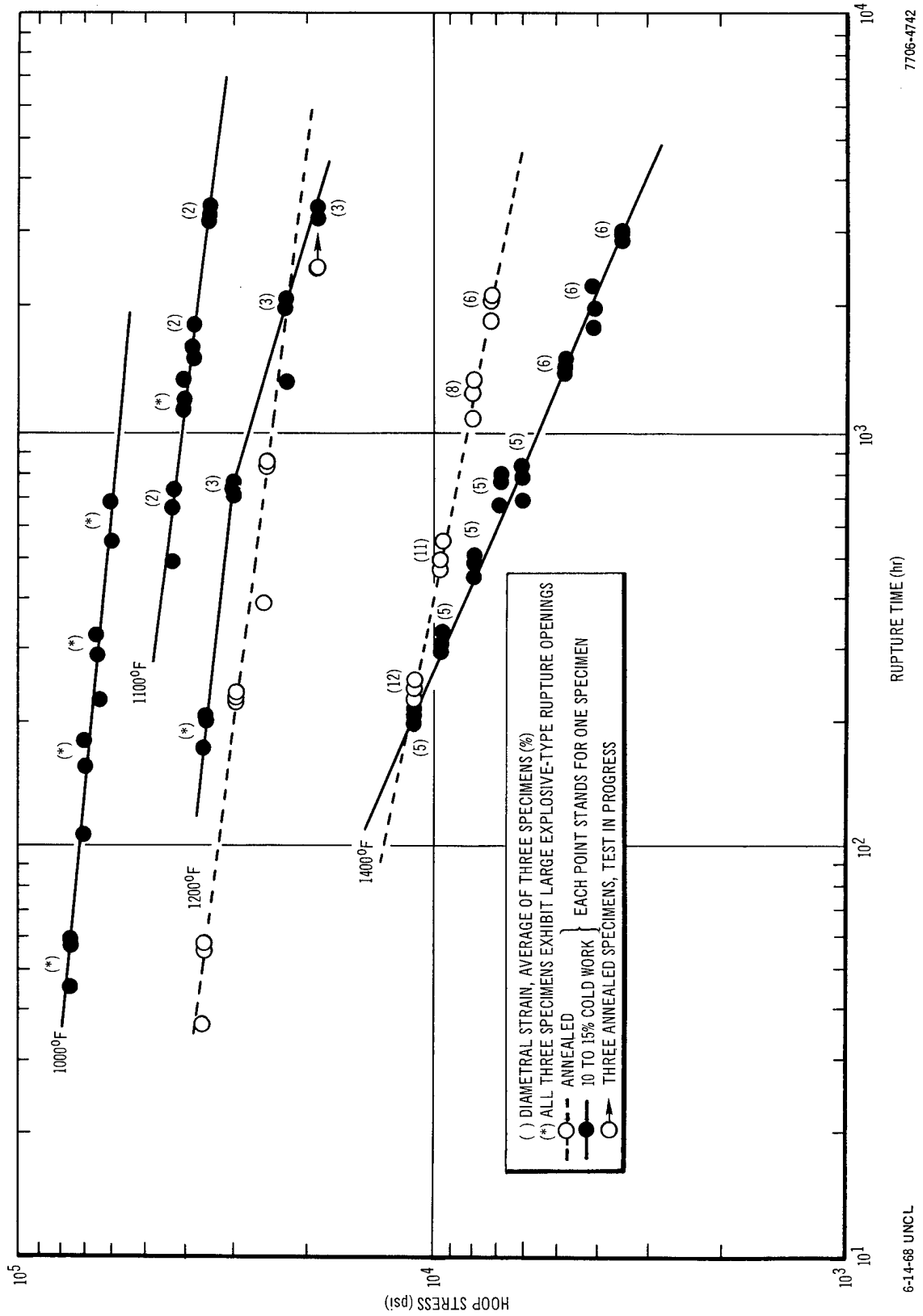

Figure 2. Biaxial Stress-Rupture Properties of Type 304 Stainless Steel in High-Purity Sodium

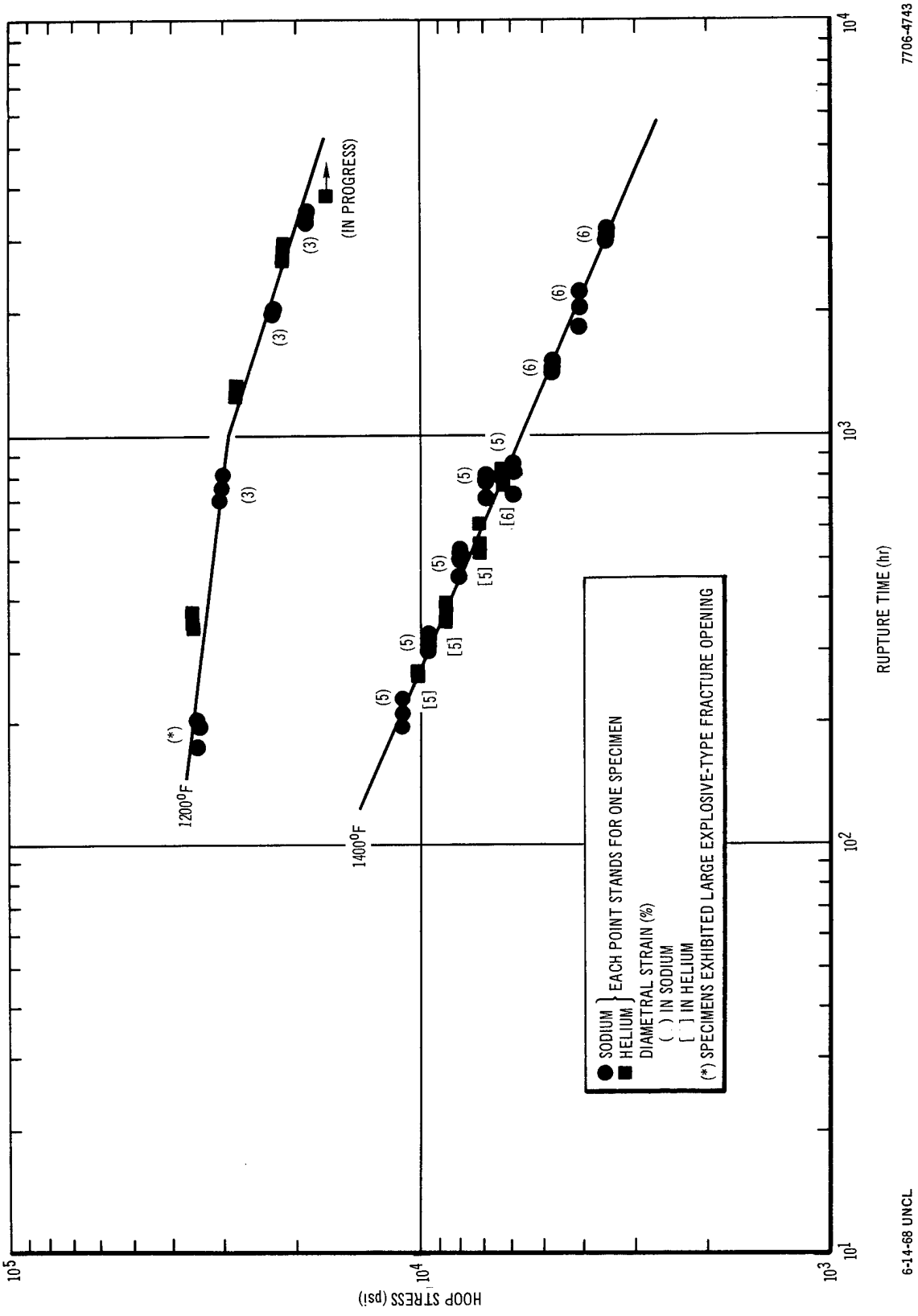

Figure 3. Biaxial Stress-Rupture Properties of 10 to 15% Cold-Worked Type 304 Stainless Steel in Sodium and Helium

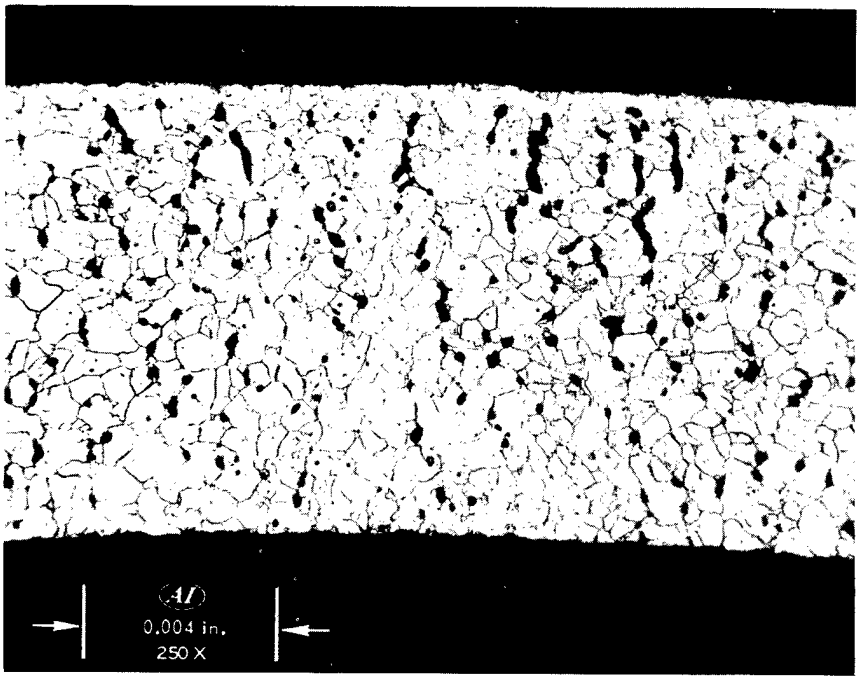

a. Stress-Rupture Tested for 813 hr (σ = 6800 psi, ϵ = 6%) (180° from rupture)

Etchant: Marble's Solution 8002-1-7

b. Biaxially Stress-Rupture Tested for 3032 hr (σ = 3500 psi, ϵ = 7%) (away from rupture)

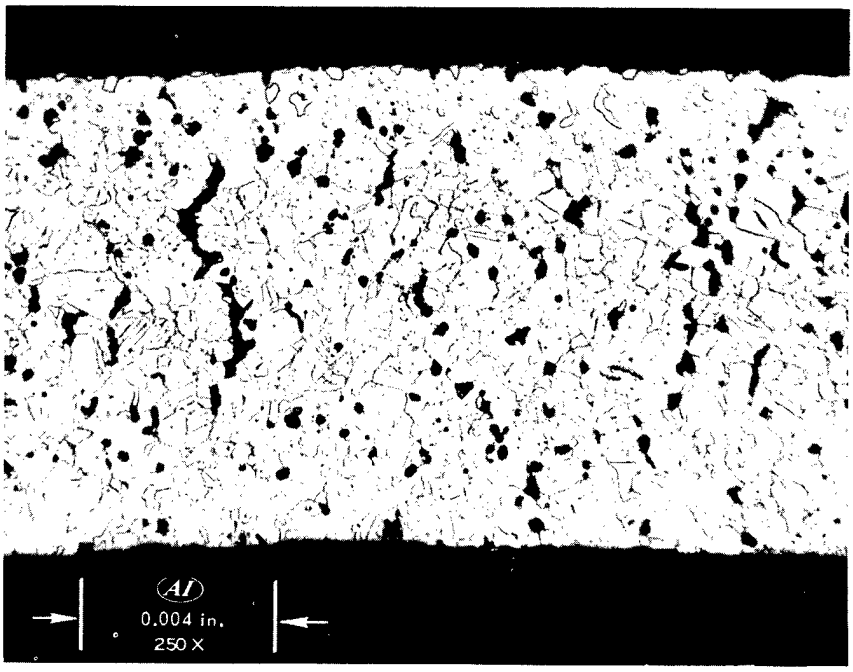

Etchant: Marble's Solution 8218-3-1

Figure 4. Type 304 Stainless Steel Tubing (10 to 15% Cold Work) Tested in 1400° F Sodium

the grain, as a result of 2200 hr exposure in the 1400°F sodium (Figure 5). A very small amount of sigma particles (<1%) was also observed on the grain boundaries, particularly in regions of greatest strain. The density of sigma particles found in the annealed tubing was much less than found in cold-worked material. Some grain-boundary migration, grain growth, and grain-boundary zone serration were also found (Figure 5a). The hardness of annealed tubing was not changed by testing.

An unstressed control specimen was soaked in the 1400°F sodium retort to determine the effect of stress on the microstructure of the annealed specimens. Its microstructure revealed distinct carbide precipitation on grain boundaries, with some grain-boundary migration and grain growth (Figure 5b). Stress appeared to cause serration of grain boundaries and to increase the amount of sigma particles formed at grain boundaries.

The microstructure of ruptured Type 304 stainless steel tubing, containing 10 to 15% cold work and tested in 1400°F high-purity helium, was compared to that of the same material tested in sodium. The specimens exhibited similar microstructures.

Metallographic examination of the cold-worked Type 304 stainless steel, ruptured in 1200°F sodium, revealed microstructures similar to those found in specimens tested in 1400°F sodium (Figure 6). However, a reduced amount of grain-boundary voids were evident. The amount and size of sigma particles on grain boundaries were also found to be reduced, when compared to those found in specimens tested at 1400°F (Figure 6b). No reaction layer was observed on the OD of tubing tested in 1200°F sodium. Slight necking on the ID of the tubing was evident (Figure 6a). The hardness was slightly reduced by 3400 hr of stress-rupture testing in 1200°F sodium (from R_c23 to R_c20).

Metallographic examination of the cold-worked Type 304 stainless steel, ruptured in 1100 and 1000°F sodium, has not been completed, and therefore will not be included in this report.

B. AISI TYPE 316 STAINLESS STEEL IN LOW-OXYGEN (~10 ppm) SODIUM

The results of 10 to 15% cold-worked and annealed Type 316 stainless steel tubing (Heat No. 65808), stress-rupture tested in 1200 and 1400°F sodium, are

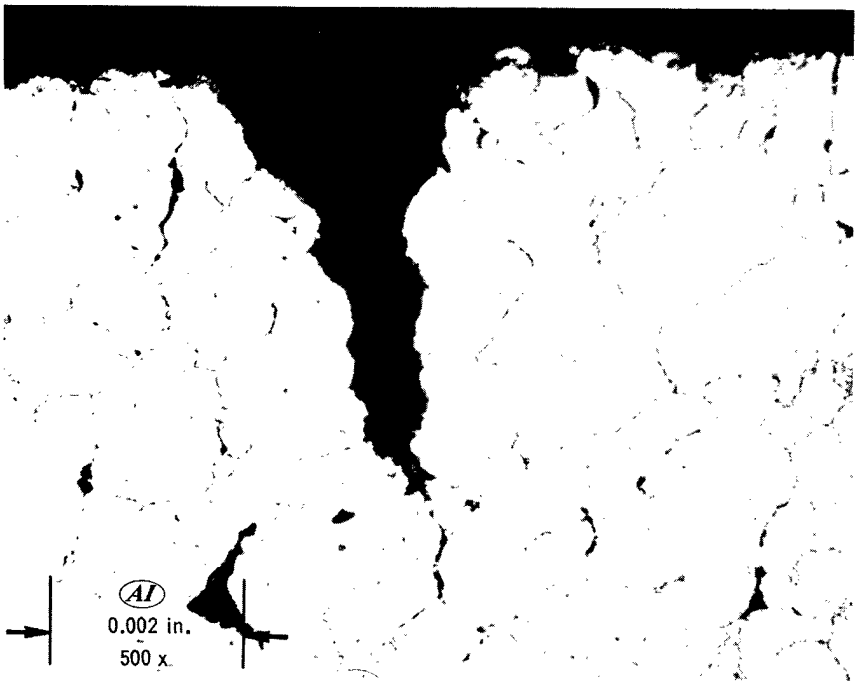

Etchant: Marble's Solution

8081-2-1

a. Stress-Rupture Tested ($\sigma = 9500$ psi, $t_r = 502$ hr, $\epsilon = 12\%$) (Note general grain boundary serration)

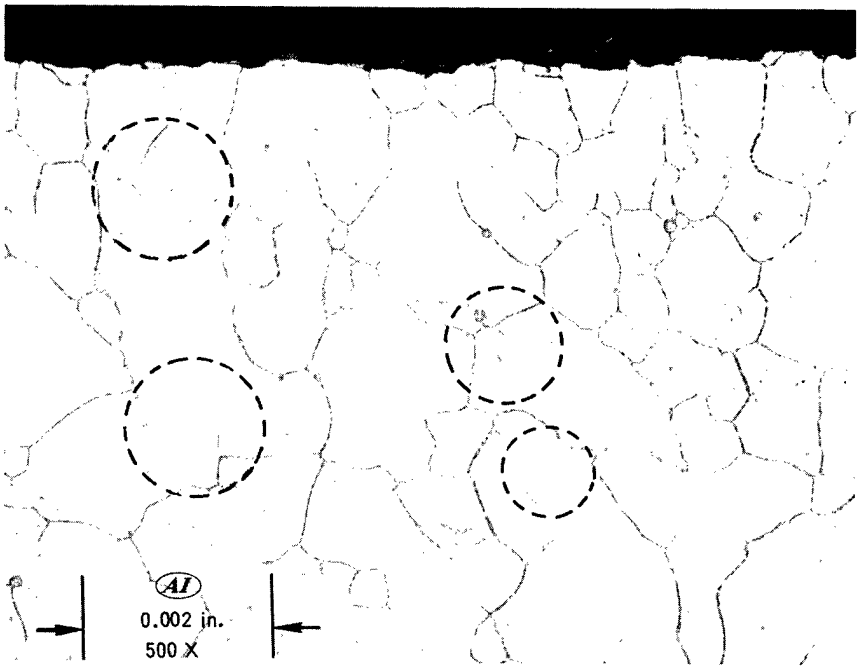

Etchant: Marble's Solution

8081-7-2

b. Soaked Without Stress for 2200 hr (Note grain boundary migration and growth)

Figure 5. Annealed Type 304 Stainless Steel Tested in 1400° F Sodium

a. Rupture Area (Note slight necking on ID)

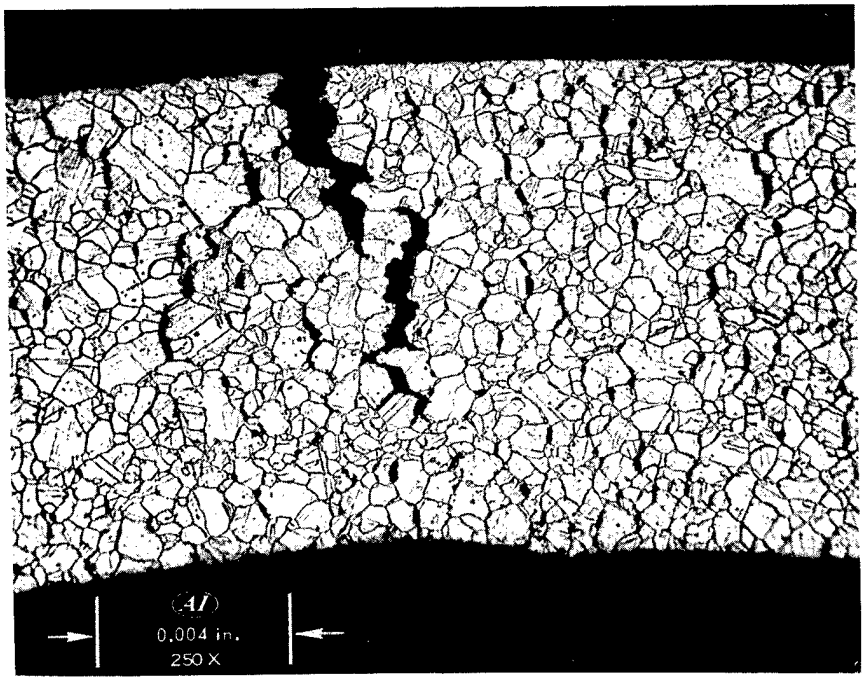

Etchant: Marble's Solution 8218-5-1

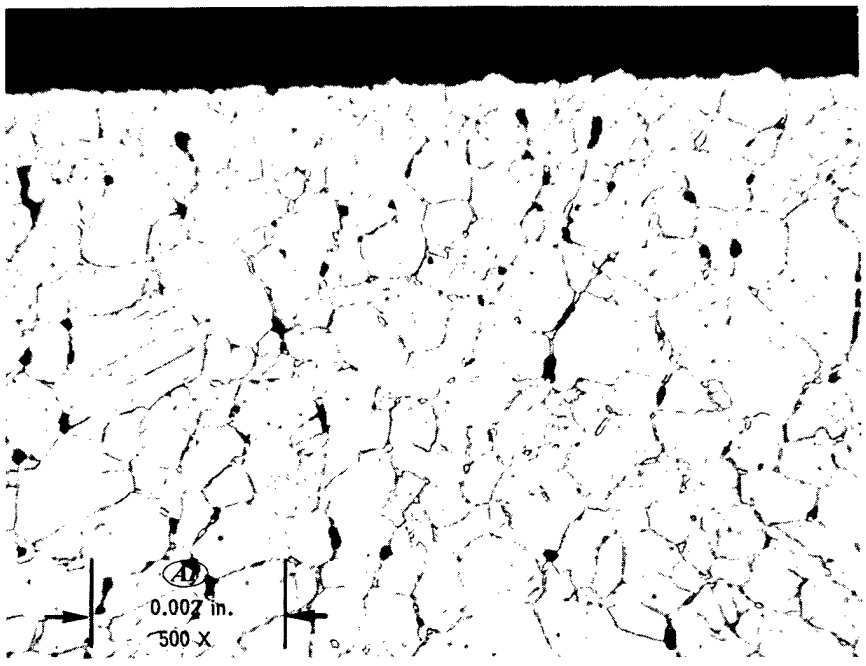

Etchant: Marble's Solution 8218-5-4

b. 180° From Rupture

Figure 6. Type 304 Stainless Steel (10 to 15% Cold Work) Tested in 1200°F Sodium (σ = 19,000 psi, t_r = 3400 hr, ϵ = 3.3%)

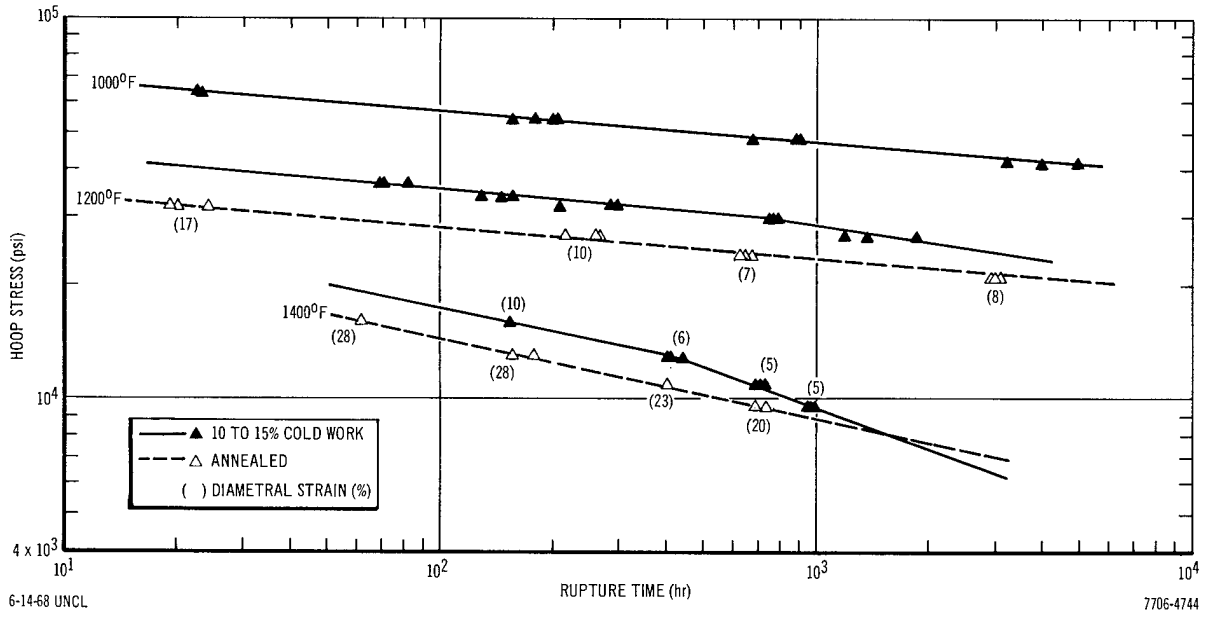

Figure 7. Biaxial Stress-Rupture Properties of Type 316 Stainless Steel in High-Purity Sodium

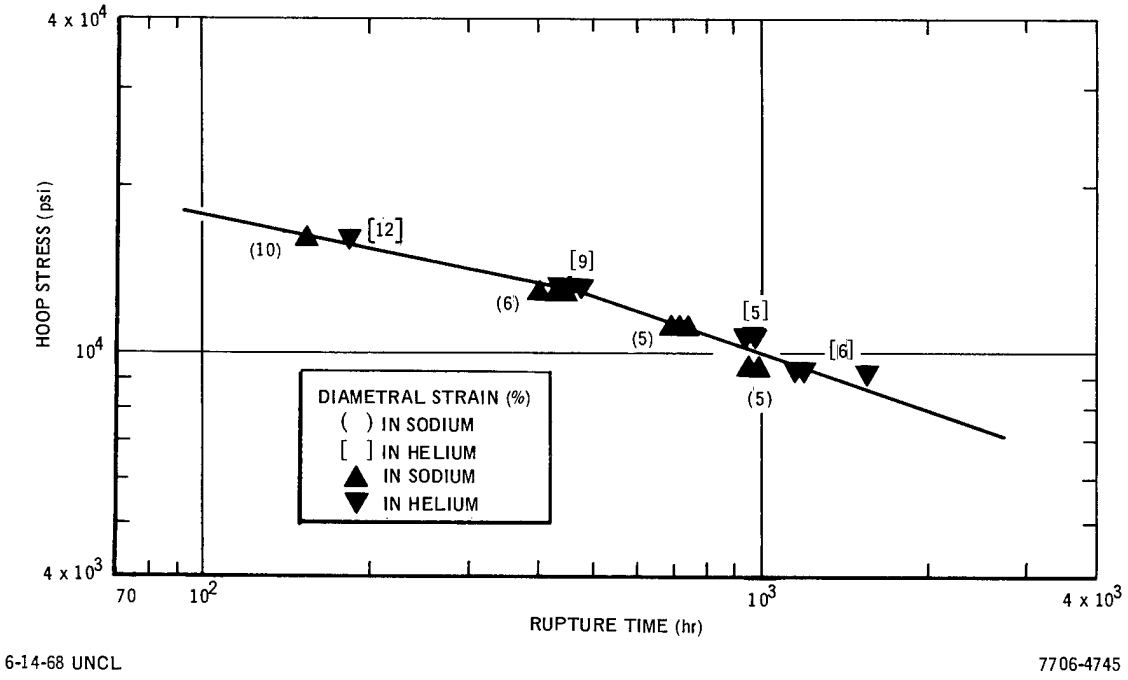

Figure 8. Stress-Rupture Properties of 10 to 15% Cold-Worked Type 316 Stainless Steel in 1400°F Sodium and Helium

summarized in Table 4 and are plotted in Figure 7. A retort, containing 12 as-received (10 to 15% cold work) Type 316 stainless steel specimens from the same heat, was tested in 1400°F high-purity helium (Figure 8). Compared with results of identical tests of annealed tubing in sodium, cold work reduced the long-term rupture strength of Type 316 stainless steel tubing at 1200 and 1400°F. Specimens from the same heat of 10 to 15% cold-worked Type 316 stainless steel, tested in high-purity sodium and helium, showed essentially the same stress-rupture strength, up to a rupture time of 1500 hr at 1400°F.

Metallographic examination of 10 to 15% cold-worked Type 316 stainless steel specimens, after rupture in 1400°F sodium, revealed intergranular failures with fissuring along grain boundaries (Figure 9b). A large quantity of fine carbide and sigma precipitates, compared to that observed in Type 304 stainless steel under a similar test temperature and time, was found on grain boundaries and on twin boundaries and slip bands within grains. Larger sigma particles were also observed on grain boundaries, particularly at triple points. Hardness of the ruptured tubing was reduced (from R_c23 to R_b89).

As-received Type 316 stainless steel (10 to 15% cold work) specimens, tested in 1400°F high-purity helium, exhibited a similar microstructure to that of the same tubing tested in 1400°F sodium. This further substantiates the conclusion that sodium has no adverse effect on the stress-rupture behavior of Type 316 stainless steel. In general, the as-received (10 to 15% cold work) Type 316 stainless steel, tested in 1200°F sodium, exhibited microstructures comparable to those found in specimens tested at 1400°F.

Microscopic examination of annealed Type 316 stainless steel tubing, tested in 1400°F sodium, revealed very few intergranular voids (Figure 9a). Large amounts of grain deformation were observed, particularly at rupture areas. An extreme case, with extensive necking at the rupture areas, is shown in Figure 10c. Large quantities of fine carbides were distributed within the grains, on grain boundaries, and on twin boundaries. Little or no sigma phase was observed in the annealed specimen tested at 1400°F in a sodium environment for 740 hr. Annealed specimens, tested in 1200°F sodium, exhibited microstructures similar to those found for 1400°F specimens. However, little or no fissures were found on grain boundaries, and no sigma phase was observed. Distinct grain growth of annealed Type 316 stainless steel, tested in 1400 and 1200°F sodium, was evident (Figures 10c and 10b).

TABLE 4
(Sheet 1 of 2)

BIAXIAL STRESS-RUPTURE DATA FOR TYPE 316 STAINLESS STEEL
(Heat No. 65808)

Alloy Condition	Environment	Temperature (°F)	Specimen Number	Hoop Stress (psi)	Rupture Time (hr)	Diametral Strain (maximum) (%)
10 to 15% Cold Work	Sodium ($O_2 \sim 10$ ppm)	1400	6-12	16,000	152	9.1
			-11	16,000	152	10.8
			-10	16,000	152	11.0
			-9	13,000	405	6.4
			-8	13,000	440	6.9
			-7	13,000	405	5.9
			-6	11,000	689	5.3
			-5	11,000	727	4.9
			-4	11,000	705	5.6
			-3	9,600	968	4.9
			-2	9,600	944	5.4
			-1	9,600	944	4.4
Annealed	Sodium ($O_2 \sim 10$ ppm)	1400	A6-12	16,000	61	26.5
			-11	16,000	61	27.7
			-10	16,000	61	29.4
			-9	13,000	176	28.4
			-8	13,000	152	27.2
			-7	13,000	152	29.9
			-6	11,000	397	22.9
			-5	11,000	397	23.7
			-4	11,000	397	22.0
			-3	9,600	731	19.5
			-2	9,600	681	20.5
			-1	9,600	681	19.1
10 to 15% Cold Work	Helium (99.99%)	1400	6-48	16,000	182	11.6
			-47	16,000	182	11.5
			-46	16,000	182	12.6
			-45	13,000	433	8.4
			-44	13,000	454	7.3
			-43	13,000	469	10.0
			-42	10,300	925	5.3
			-41	10,300	925	4.6
			-40	10,300	963	5.8
			-39	9,300	1123	8.7
			-38	9,300	1142	5.4
			-37	9,300	1549	5.4

TABLE 4
(Sheet 2 of 2)

BIAXIAL STRESS-RUPTURE DATA FOR TYPE 316 STAINLESS STEEL
(Heat No. 65808)

Alloy Condition	Environment	Temperature (°F)	Specimen Number	Hoop Stress (psi)	Rupture Time (hr)	Diametral Strain (maximum) (%)
10 to 15% Cold Work	Sodium ($O_2 \sim 10$ ppm)	1200	6-79	37,000	81	In Progress
			-78	37,000	67	In Progress
			-77	37,000	68	In Progress
			-76	34,000	129	In Progress
			-75	34,000	143	In Progress
			-74	34,000	153	In Progress
			-73	32,000	206	In Progress
			-72	32,000	292	In Progress
			-71	32,000	276	In Progress
			-70	27,000	1822	In Progress
			-50	27,000	1354	In Progress
			-49	27,000	1189	In Progress
Annealed	Sodium ($O_2 \sim 10$ ppm)	1200	A6-24	32,000	24	15.9
			-23	32,000	20	17.8
			-22	32,000	19	16.6
			-21	27,000	214	10.4
			-20	27,000	264	10.6
			-19	27,000	259	10.1
			-18	24,000	645	7.4
			-17	24,000	621	7.6
			-16	24,000	681	7.2
			-15	21,000	3054	7.6
			-14	21,000	2958	8.5
			-13	21,000	3006	8.5
10 to 15% Cold Work	Sodium ($O_2 \sim 10$ ppm)	1000	6-36	64,000	23	In Progress
			-34	64,000	23	In Progress
			-33	54,000	206	In Progress
			-32	54,000	152	In Progress
			-31	54,000	176	In Progress
			-30	48,000	674	In Progress
			-29	48,000	875	In Progress
			-28	48,000	898	In Progress
			-27	42,000	3970	In Progress
			-26	42,000	4884	In Progress
			-25	42,000	3170	In Progress

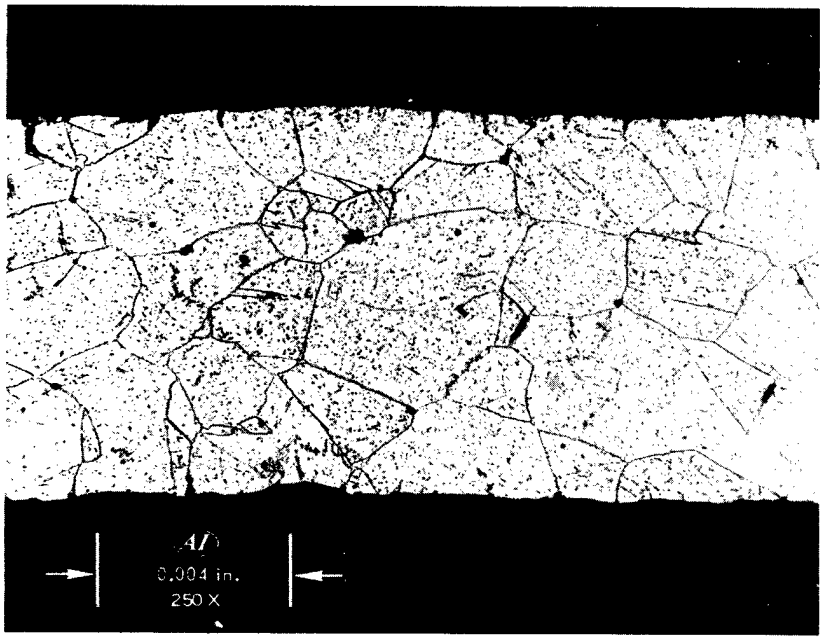

a. Annealed (σ = 9600 psi, t_r = 731 hr, ϵ = 19.5%)

Etchant: Marble's Solution

8180-7-1

b. 10 to 15% Cold Work (σ = 13,000 psi, t_r = 405 hr, ϵ = 6%)

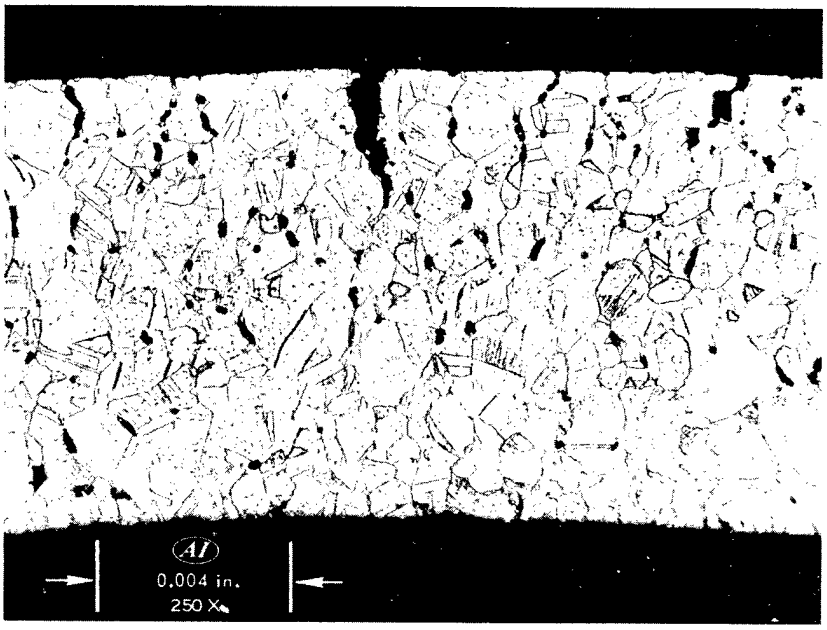

Etchant: Marble's Solution

8094-1-2

Figure 9. Effect of Cold Work on Microstructure and Void Density of Type 316 Stainless Steel Stress-Rupture Tested in 1400°F Sodium

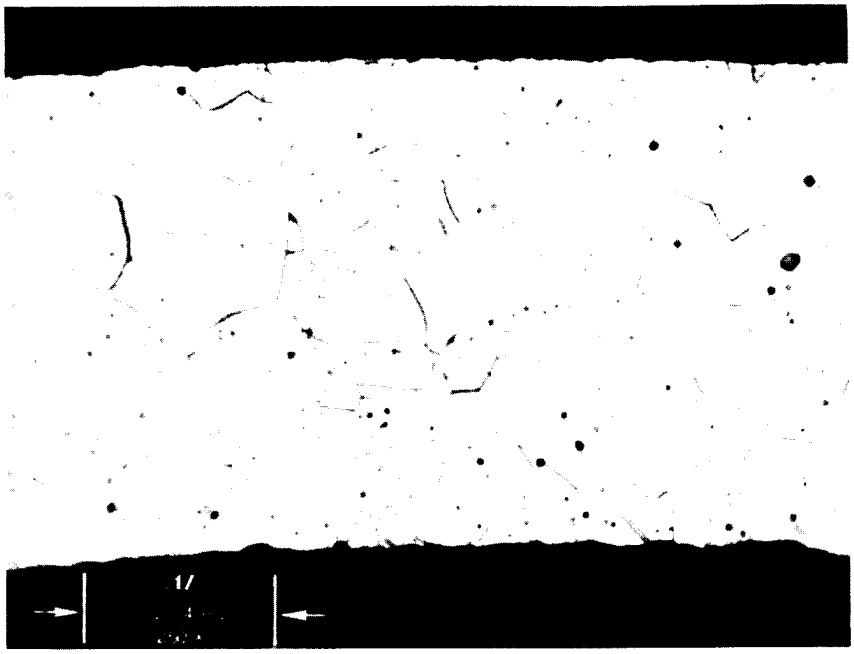

Etchant: Marble's Solution 8226-2-1

a. As-Received

Etchant: Marble's Solution 8182-8-1

1) Rupture Area (Note grain deformation)

Etcha

c. Tested in 1400° F Sodium for 970 hr (σ = 16,0

Etchant: Marble's Solution 8239-4-1

b. Tested in 1200° F Sodium for 3100 hr (σ = 21,000 psi, t_r = 2958 hr, ϵ = 8.5%)

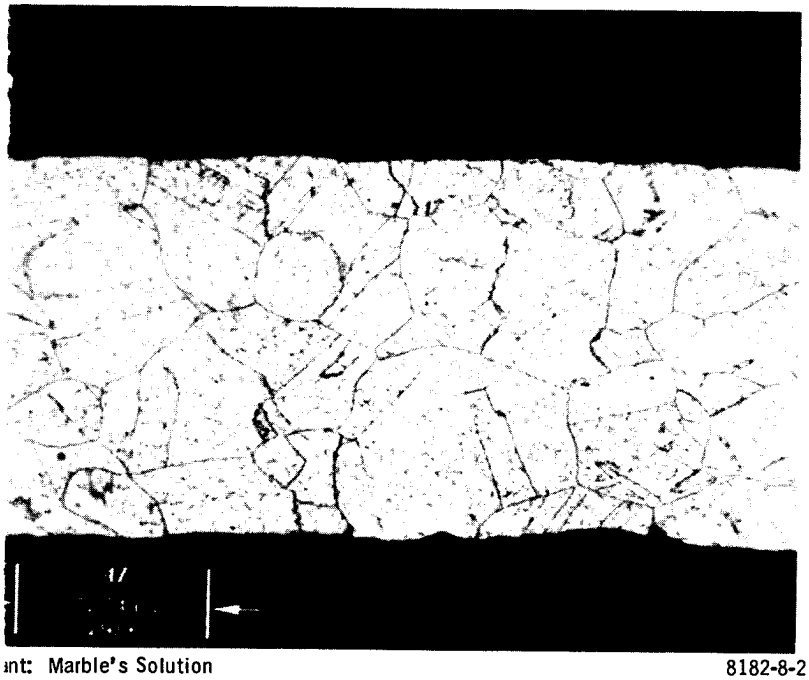

ınt: Marble's Solution 8182-8-2

2) 180° From Rupture (Note absence of grain boundary voids)

00 psi, t_r = 61 hr, ϵ = 29%)

Figure 10. Annealed Type 316 Stainless Steel

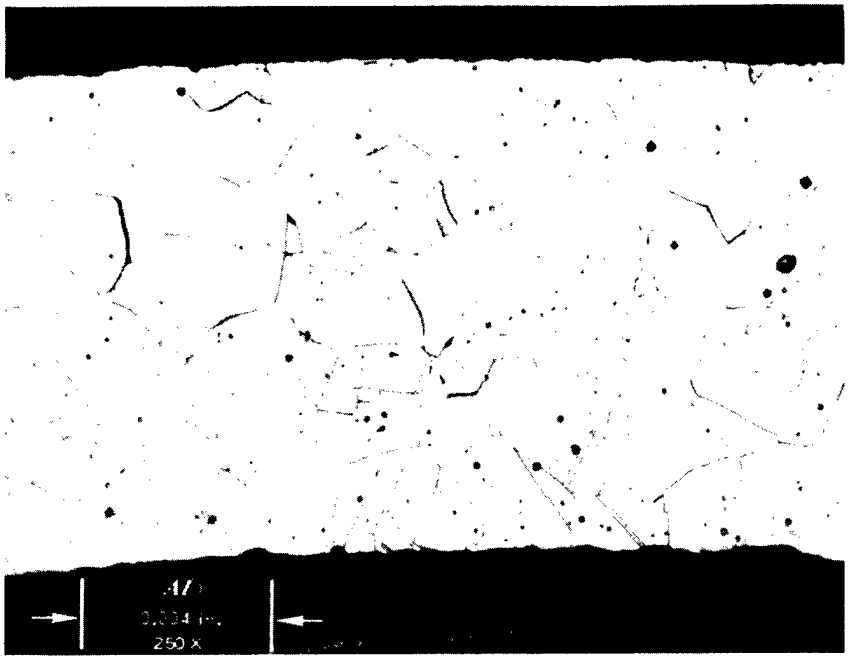

a. As-Received

Etchant: Marble's Solution 8226-2-1

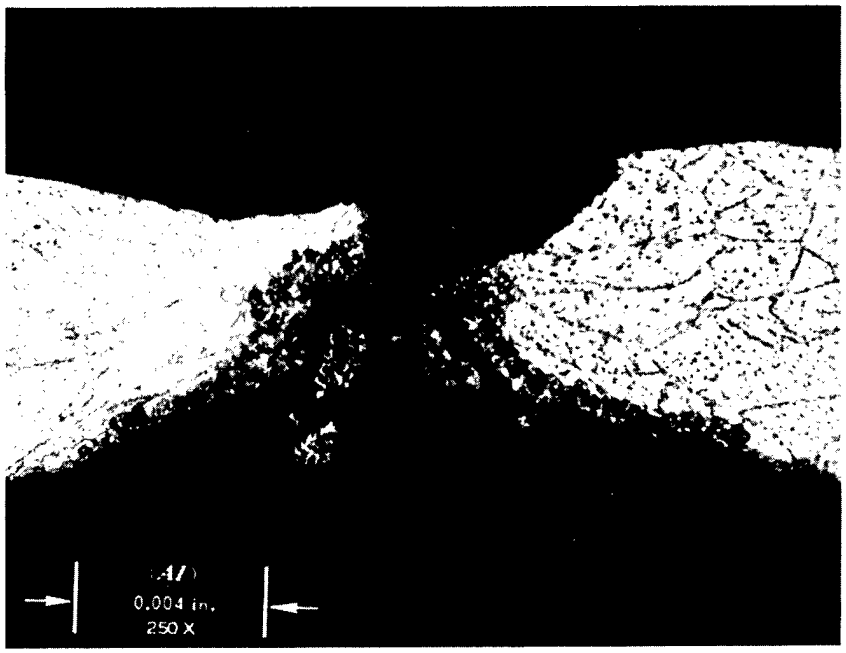

Etchant: Marble's Solution 8182-8-1

1) Rupture Area (Note grain deformation)

Etcha

c. Tested in 1400° F Sodium for 970 hr (σ = 16,0

IV. DISCUSSION

A. MECHANICAL PROPERTIES

Four observations were made concerning the stress-rupture behavior of cold-worked Types 304 and 316 stainless steel, tested in a high-purity static sodium environment at 1200 and 1400° F:

1) The stress-rupture behavior of as-received (10 to 15% cold work) material at 1200 and 1400° F in high-purity sodium is comparable to the strength obtained in high-purity helium (Figures 3 and 8).

2) The presence of internal stresses in the 10 to 15% cold-worked tubing appears to have no effect on the biaxial stress-rupture properties of austenitic stainless steels in high-purity liquid sodium environment.

3) The slope of the long-term stress-rupture curve for as-received (10 to 15% cold work) material is steeper than that of annealed material from the same heat (Figures 2 and 7). This behavior of material, due to cold work, has been reported for uniaxial tests in the literature.[10,11]

4) At 1400 and 1200° F, the 10 to 15% cold-worked Type 316 stainless steel exhibited significantly higher long-term rupture strength than the 10 to 15% cold-worked Type 304 stainless steel (shown later, in Figure 16). The rupture strength of 10 to 15% cold-worked Type 316 stainless steel, however, is lower than that of 10 to 15% cold-worked Type 304 stainless steel tested for 1000 hr in 1000° F sodium. In the annealed condition, Type 316 stainless steel exhibits a slightly higher long-term rupture strength, when compared to Type 304 stainless steel. Annealed Type 316 stainless steel possesses superior ductility ($\Delta D/D_0$), when compared to its cold-worked form, annealed Type 304 stainless steel, and cold-worked Type 304 stainless steel, when tested under similar temperature and time conditions (shown later, in Figure 15).

To demonstrate the consistency of the material behavior over a range of temperatures and times, Larson-Miller parameters for stress-rupture data of

Figure 11.

Larson-Miller Master Parameter Curve for 10 to 15% Cold-Worked Type 304 Stainless Steel

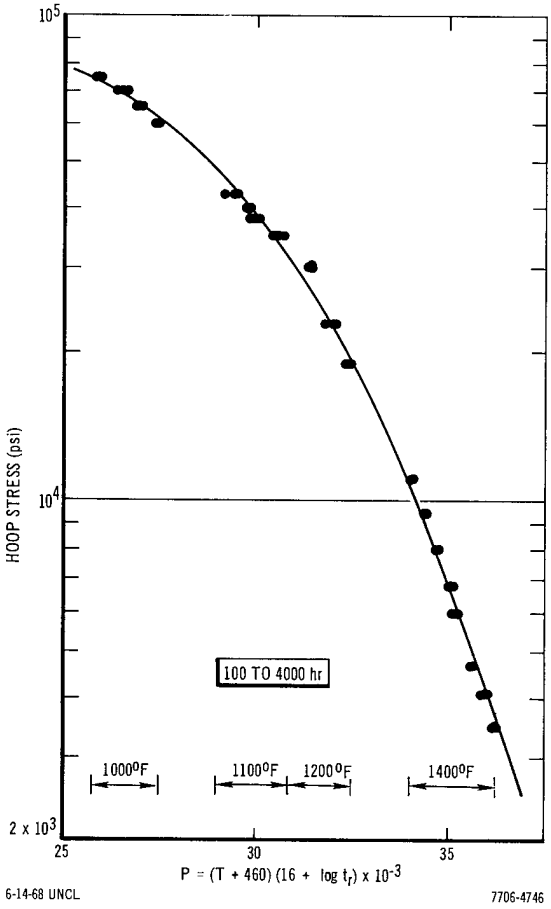

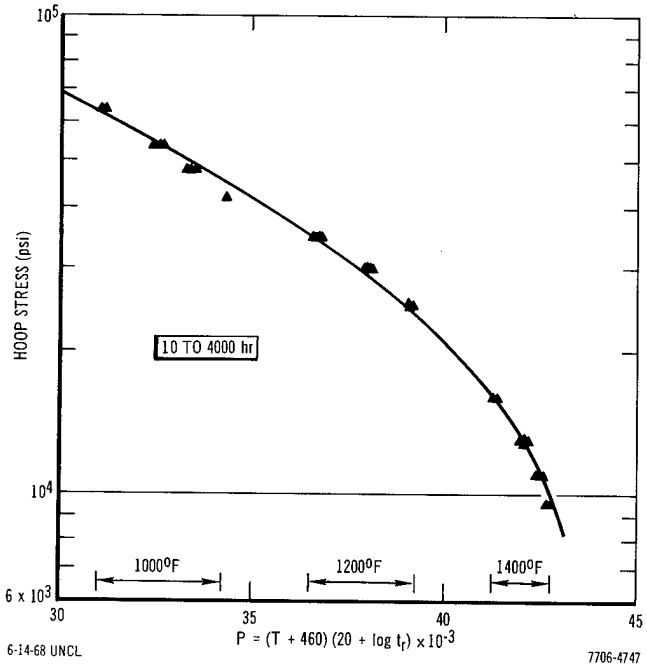

Figure 12.

Larson-Miller Master Parameter Curve for 10 to 15% Cold-Worked Type 316 Stainless Steel

10 to 15% cold-worked Types 304 and 316 stainless steel are plotted in Figure 11 and Figure 12, respectively. A material constant of 16 was calculated from the experimental data for 10 to 15% cold-worked Type 304 stainless steel, resulting in a Larson-Miller equation of

$$P = (T + 460)(16 + \log t_r) \quad , \qquad \ldots(2)$$

where

P = Larson-Miller parameter

T = temperature (°F)

t_r = rupture time (hr).

Similarly, the Larson-Miller equation for 10 to 15% cold-worked Type 316 stainless steel is represented by

$$P = (T + 460)(20 + \log t_r) \qquad \ldots(3)$$

In this case, the material constant (C) is assumed to be 20,[12] since there was insufficient data to calculate the constant. In general, the use of such an empirical relationship should allow for reasonably accurate extrapolations of material strength to temperatures and times not covered by experimental data. However, reliable extrapolations of rupture data to prolonged times and higher temperatures require the absence of changes in slope in the log stress vs log rupture life curve. This slope change is found in the Type 304 and Type 316 stainless steel data, as shown in Figures 2 and 7, respectively.

It is apparent, from the data presented in Figures 3 and 8, that the high-purity static sodium environment has no significant effect on the mechanical properties of either austenitic stainless steel, tested for periods up to 1000 and 3000 hr at 1400 and 1200°F, respectively. Also, no significant embrittlement effect, due to 1400°F sodium, on either austenitic stainless steel is found (Figure 13). As is illustrated in Figure 14, no significant effect of 1400°F sodium environment on the strain-rate (maximum diametral strain/rupture time) behavior of either 10 to 15% cold-worked Type 304 or Type 316 stainless steel is apparent. Comparable microstructural characteristics of the ruptured tubing from 1400°F sodium and helium environments further substantiate these findings. Similar observations on austenitic stainless steels in 1200°F clean sodium have been reported in the literature.[6]

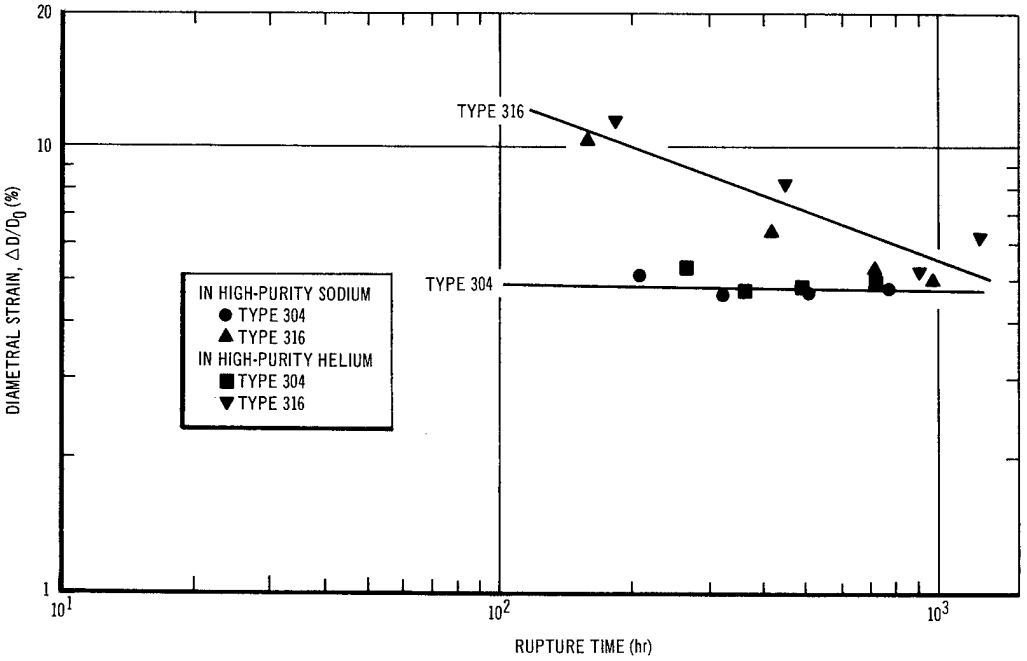

Figure 13. Effect of Environments on Strain Behavior of 10 to 15% Cold-Worked Types 304 and 316 Stainless Steels at 1400°F

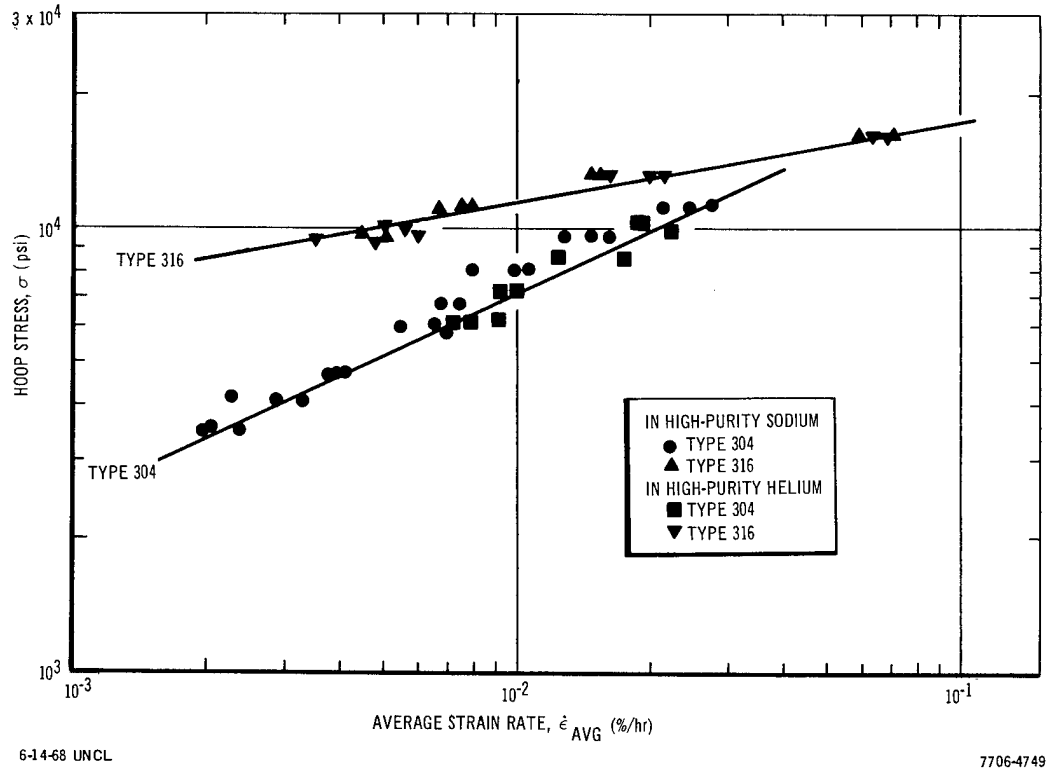

Figure 14. Effect of Environments on Strain-Rate Behavior of 10 to 15% Cold-Worked Types 304 and 316 Stainless Steels at 1400°F

As has been noted by Rostoker et al.,[7] cold-worked material, tested in a liquid metal environment, may exhibit severe degradation of mechanical properties, when compared to its annealed counterpart. It is conceivable that internal stresses could enhance premature fracture, due to intercrystalline penetration by liquid metal.[1] However, from the data obtained in this research, no observable grain-boundary penetration of liquid sodium or degradation of mechanical properties was found that could be attributed to the presence of internal stresses in the 10 to 15% cold-worked austenitic stainless steel tubing. As a result of the data presented, therefore, high-purity static liquid sodium appears to have no significant effect on either the 10 to 15% cold-worked or the annealed austenitic stainless steels.

The long-term stress-rupture curves of cold-worked tubing have a steeper slope than those for annealed material. Although the cold-worked material has higher short-term rupture strength, the two curves converge and cross, with the annealed material possessing superior long-term rupture strength. The cold-work effect is particularly pronounced in Type 304 stainless steel tested at 1400°F. Specifically, while the "crossover" points for Type 304 stainless steel, tested at 1400 and 1200°F, are around 200 and 1300 hr, respectively, the crossover points for Type 316 stainless steel, tested at similar temperatures, are around 1600 and 30,000 hr (extrapolated value for 1200°F data), respectively. The decrease in time for the crossover point to occur with an increase in temperature is attributed to the increase of the rate of recovery or relaxation of internal elastic stresses in the cold-worked material. The crossover point for Type 316 stainless steel occured in a much longer time, when compared to Type 304 stainless steel, for testing at a similar temperature. This is probably caused by the presence of molybdenum in Type 316 stainless steel, since molybdenum tends to increase the stability of austenitic stainless steel,[13] lowering the rate of recovery and recrystallization. Work by Krebs and Soltys (uniaxial tests) on Type 304 stainless steel,[11] and by Richardson and McDowell[10] on M316 alloy (biaxial tests), show similar stress-rupture behavior.

The break in the stress-rupture curve can be attributed to several factors:

1) Change of fracture process from a transgranular to an intergranular fracture[11]

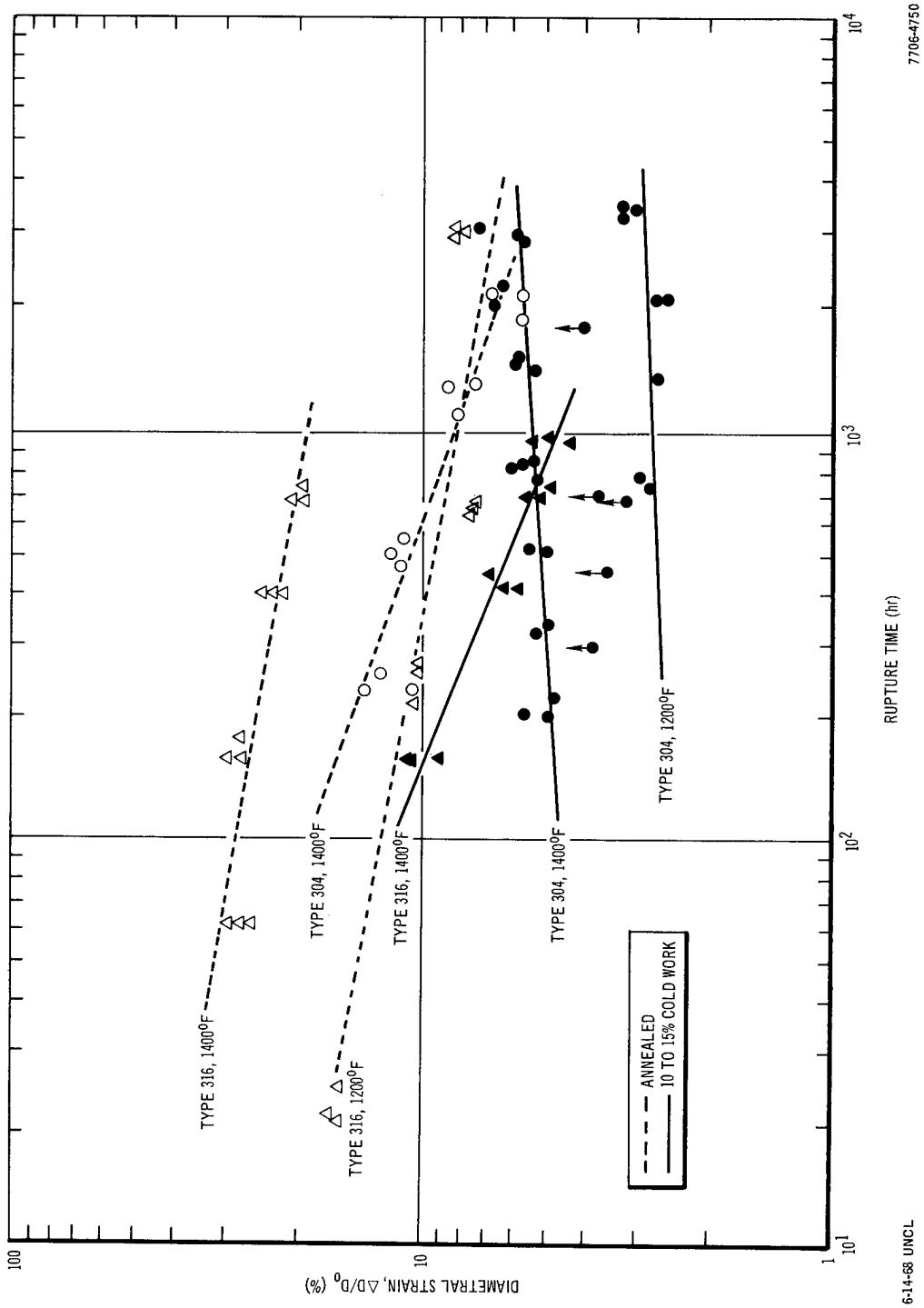

Figure 15. Strain Variation With Rupture Time for 10 to 15% Cold-Worked Types 304 and 316 Stainless Steels in 1200 and 1400°F Sodium

2) Recrystallization[15]

3) Precipitation.[16]

Since the test temperatures were above the equicohesive temperatures of both austenitic stainless steels at the low strain rates, grain boundaries are regions of weakness and could give rise to intergranular failures. All ruptures in the cold-worked Types 316 and 304 stainless steel were found to be intercrystalline. Further comparison of the microstructures of the tested specimens, before and after the break points (in log stress vs log time curve), reveal no observable differences. Due to the design features of the test retort, ruptured specimens could not be removed from the retort individually without terminating the entire test; therefore, all specimens were exposed to the same temperature for the same length of time. As a result, any contribution to phase change or precipitation by stress would have been overshadowed by the effect of thermal aging. However, it is reasonable to surmise that the break is essentially attributable to recovery and recrystallization of the cold-worked material, and possibly due to the precipitation and subsequent growth of second-phase particles on grain boundaries, since all fissures found were associated with carbide and sigma particles. Both types of second-phase particles have been reported to be sites of void nucleation and crack growth.[3,17]

Variation of diametral strain ($\Delta D/D_0$) with rupture time for Types 304 and 316 stainless steel, tested in 1200 and 1400°F sodium, is shown in Figure 15. As can be seen from the figure, cold work reduced the rupture strain significantly for both austenitic stainless steels. The rupture strain of cold-worked Type 304 stainless steel increases as the rupture time increases. This behavior is attributed to the recovery process, and probably to the growth of sigma particles, caused by the diffusion of chromium atoms away from carbides. The reduction of rupture strain with a reduction of test temperature is also consistent with the thermally-activated recovery process (Figure 15). Since the strain of the annealed and the 10 to 15% cold-worked Type 304 stainless steel approach a common value, it would appear that cold work effects disappear in about 2500 hr, when stress-rupture tested at 1400°F. Similar convergent behavior of strain to a common value for annealed and cold-worked M316 stainless steel has also been reported.[10] In these tests, however, the variation of the rupture-strain behavior of 10 to 15% cold-worked Type 316 stainless steel, tested in 1400°F

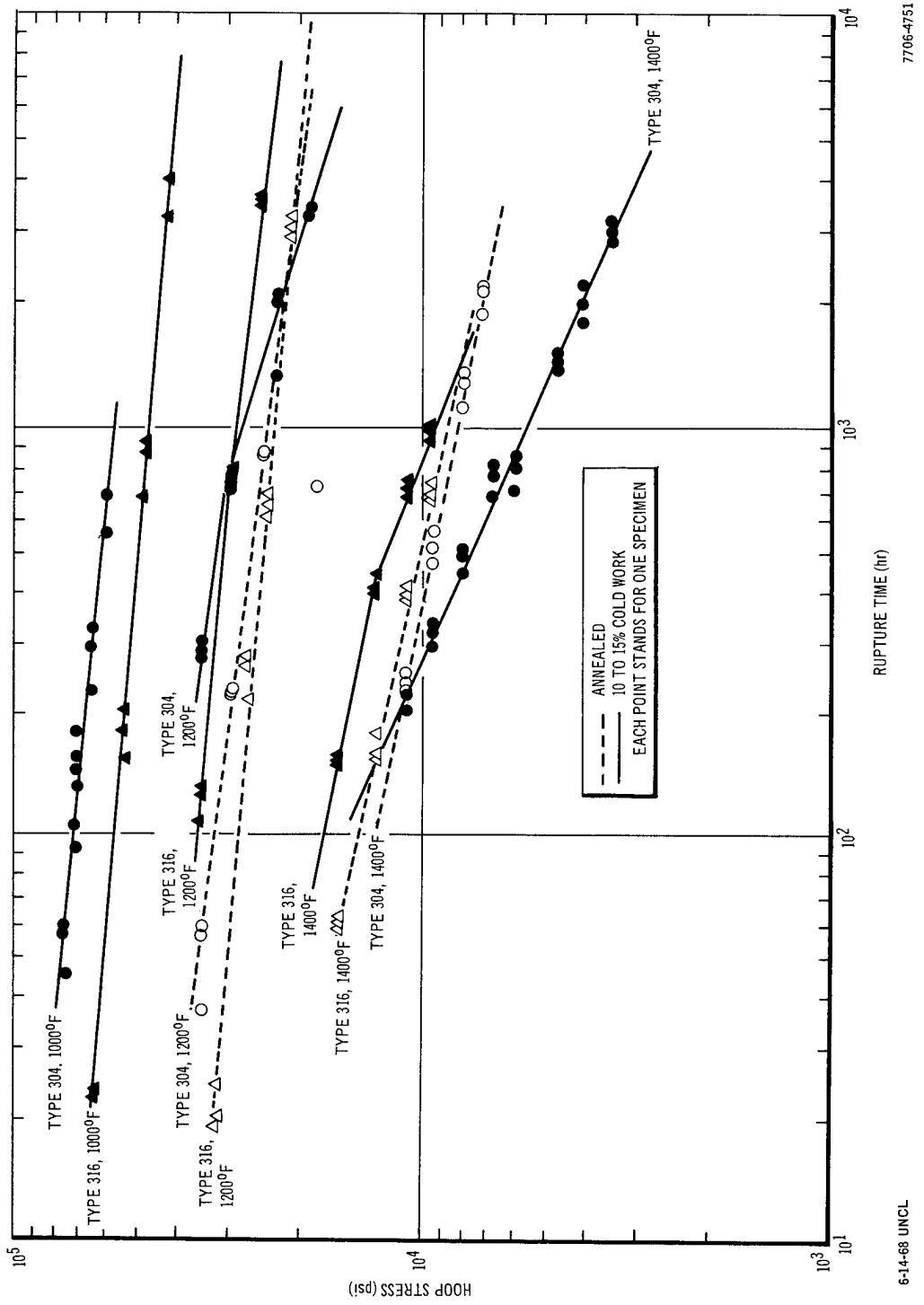

Figure 16. Stress-Rupture Properties of Types 304 and 316 Stainless Steels in 1000, 1200, and 1400°F Sodium

sodium, with rupture time is parallel to that of annealed material, and decreases as time to rupture increases. The difference in strain variation with rupture time between cold-worked Types 304 and 316 stainless steel is probably attributable to the finer and more copious dispersion of carbides and sigma phase in the Type 316 stainless steel grain matrix and sigma phase in the grain boundaries, which reduces softening and retards grain-boundary migration. The increase in recrystallization temperature and stability for Type 316 stainless steel, due to the presence of molybdenum, might also play a role.

A comparison of rupture strengths for Types 304 and 316 stainless steel reveals that the long-term rupture strength of 10 to 15% cold-worked Type 316 stainless steel is significantly higher than that for 10 to 15% cold-worked Type 304 stainless steel, tested at 1400°F (Figure 16). But this difference in rupture strength decreases as test temperature decreases. Specifically, at 1400°F, the 1000-hr rupture strength for cold-worked Type 316 stainless steel is 70% higher than that for cold-worked Type 304 stainless steel. At 1200°F, the 1000-hr rupture strength for cold-worked Type 316 is only 4% higher. At 1000°F, the 1000-hr rupture strength of cold-worked Type 316 is 20% lower than that for Type 304. The change of comparative behavior, as a function of temperature, appears to be a result of the decreased rates of precipitation and agglomeration of second-phase particles (sigma and carbides) in Type 304 stainless steel when the test temperature was reduced. Dislocation mobility determines the creep resistance of the material, and critical coherent precipitation is very effective in increasing creep resistance. However, when such materials are used at increasing temperatures to the point of instability, the precipitates tend to lose coherency and agglomerate to larger particles, losing their effectiveness in impeding dislocation motion. The agglomeration or growth of sigma particles in Type 304 stainless steel is shown in Figures 4, and later, in Figure 20.

B. EFFECT OF COLD WORK

The strengthening effect of cold work for the short-term rupture test is attributed to strain hardening, due to slip band formation, dislocation tangles, and coherent precipitation hardening within the grains. As test time increases in the creep process, the effect of strengthening by cold work decreases by:

1) The softening effect due to recovery or recrystallization of the cold-worked material

2) The growth of incoherent precipitates to an undesirable size[18]

3) The early inception of grain boundary voids, due to the weakened grain boundary from prior cold deformation and precipitation.[13]

It is proposed, by Siegfried,[13] that the cohesive strength of a material decreases as a function of time for a constant temperature and structure. The precipitation process further lowers the cohesive strength of the material under creep testing.[13] As a result, the long-term rupture strength of the cold-worked material is less than that of the annealed material.

It is proposed, by Dorn et al.,[19] that the creep rate of a polycrystalline alloy, tested at high temperature, can be represented by

$$\dot{\epsilon} = D_0(\sigma)^n \exp(-Q/RT) \quad , \qquad \ldots(4)$$

where

n and D_o = constants

σ = applied stress

Q = activation energy for creep

R = gas constant

T = absolute temperature.

Under a constant stress condition, the creep-rate equation can be simplified to

$$\dot{\epsilon} = D\exp(-Q/RT) \quad , \qquad \ldots(5)$$

where

$D = D_0(\sigma)^n$ = constant.

Assuming that the activation energy for creep is approximately insensitive to temperature in the range between 1200 and 1400°F, Equation 5 can be rearranged to calculate the activation energy (Q):

$$Q = \frac{R \ell n \frac{\dot{\epsilon}_{T_1}}{\dot{\epsilon}_{T_2}}}{\left(\frac{1}{T_2} - \frac{1}{T_1}\right)} \text{ (cal/mole)} \quad . \qquad \ldots(6)$$

From the data obtained for 10 to 15% cold-worked Type 304 stainless steel, stress-rupture tested in sodium, the activation energy (Q) was calculated to be 78 kcal/mole, a value approaching the activation energy for self-diffusion of γ-Fe.[20] Under similar biaxial stress-rupture testing conditions, Venard obtained a value of 110 kcal/mole for the activation energy for creep of annealed Type 304 stainless steel in air.[21] As a result, based on these data, cold work appears to have reduced the activation energy for creep by about 32 kcal/mole. The high-temperature (1200 to 1400°F) creep of the 10 to 15% cold-worked Type 304 stainless steel is controlled by dislocation climb mechanisms, since it gives an activation energy for creep almost equal to that for self-diffusion in γ-Fe. The high activation energy for creep of annealed Type 304 stainless steel, as obtained by Venard, suggests that the locking of dislocations by solute atoms plays a dominant role.[19]

It is not surprising to find that cold work causes a reduction of activation energy for creep. Cold working has been shown to result in the storage of energy in a metal,[22] thus increasing its potential energy. The cold-worked material may then be represented by the metastable position on the energy curve, as shown in Figure 17. The annealed condition may be represented by the stable position. When the amount of cold work increases, more energy is stored in the material, thus moving the metastable position to a higher potential energy level. Assuming the potential level of the energy barrier is constant, a smaller activation energy (Q) would be required to enable the atoms in the metastable state to pass over the energy hump to the stable state. As cold work is increased, less additional energy (activation energy) is required from other sources (e.g., thermal energy) to bring about the transfer. Experimental proofs for reduction of activation energy have been reported.[23-25] Some unpublished data on the effect of cold work on uniaxial creep-rupture properties of Type 304 stainless steel sheet in 1200°F sodium also substantiate the activation energy reduction due to cold work.[26] The reduction of activation energy is reflected by the increase in the steepness of the slope of the log stress vs log strain rate curve caused by cold work (Figure 18). The strain-rate behavior for Type 316 stainless steel at 1400°F is seen to be less affected by cold working; the cold-worked Type 316 stainless steel strain-rate curve is almost parallel to the annealed Type 316 stainless steel curve.

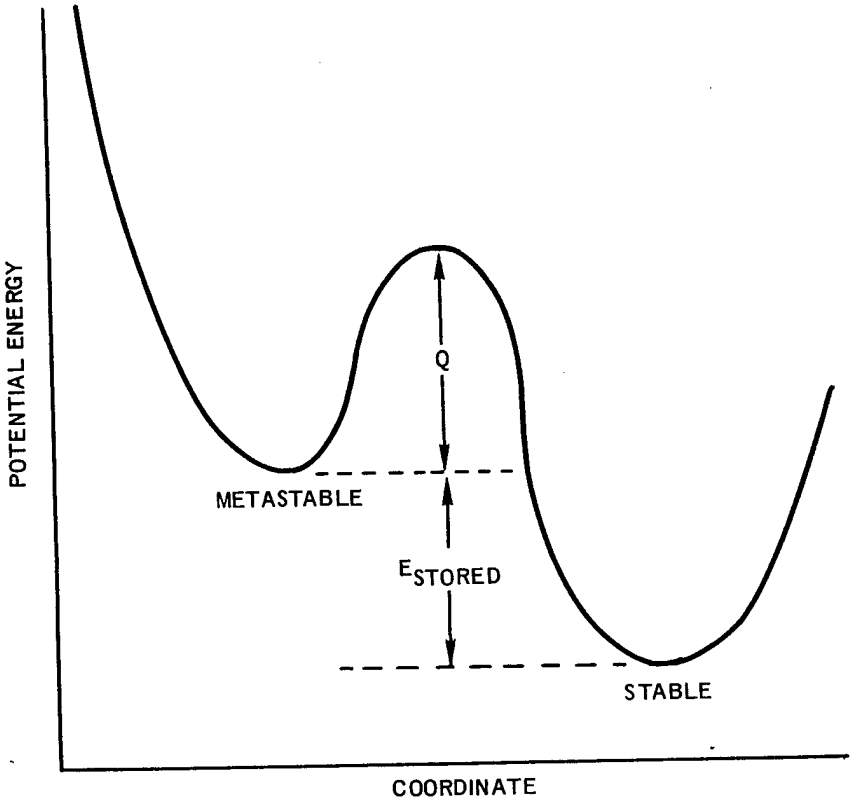

6-14-68 UNCL

7706-4752

Figure 17.

Stored Energy Due to Cold Work

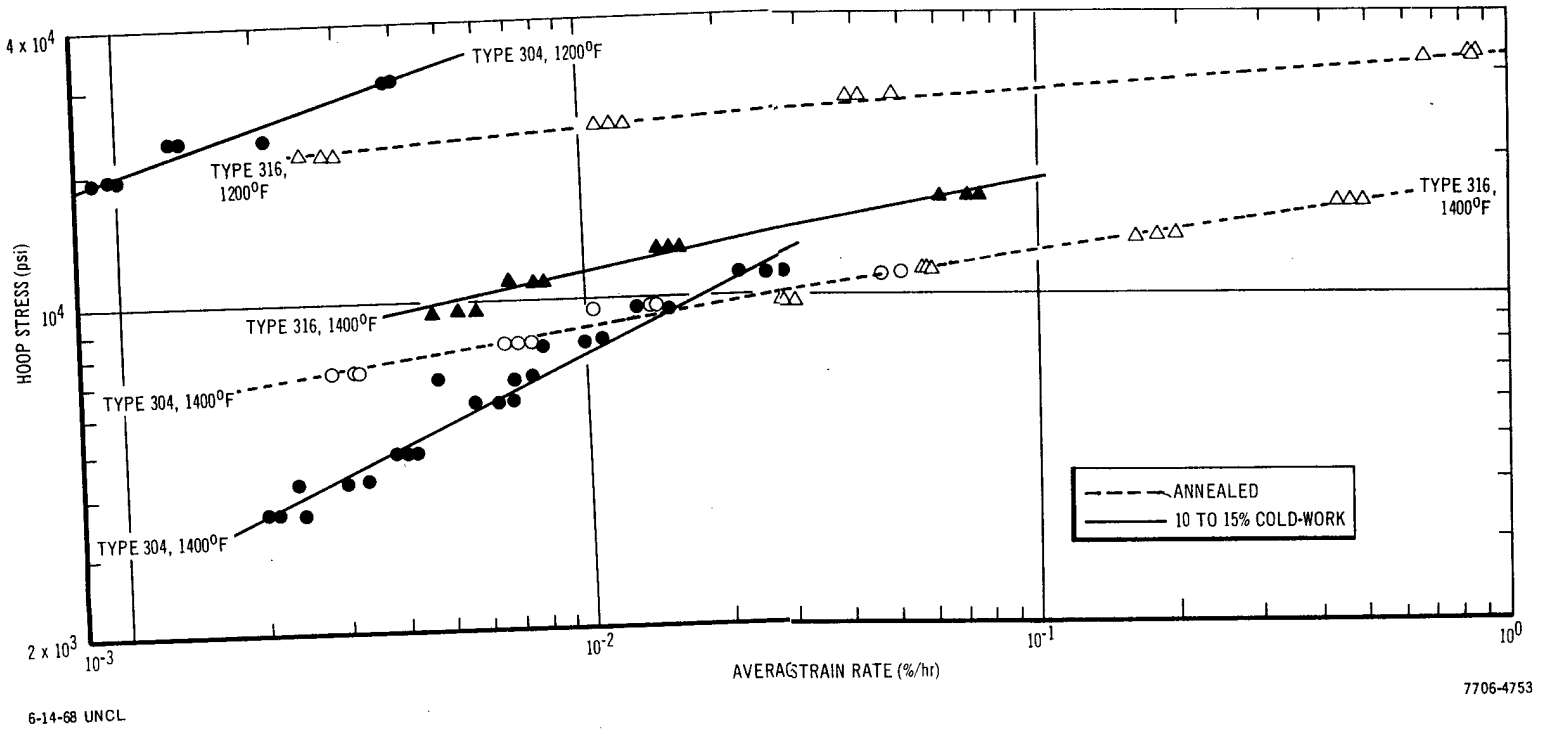

Figure 18. Variation of Strain Rate With Stress for Types 304 and 316 Stainless Steels in 1100 and 1400°F Sodium

C. SIGMA PHASE FORMATION

In addition to the extensive carbide precipitation on slip bands, twin boundaries, and grain boundaries, a second phase is also found randomly on grain boundaries, particularly in cold-worked specimens tested at 1400°F. Some of these precipitates are also found in the cold-worked Type 316 stainless steel grain matrix. This second phase was identified to be sigma phase, by selective etching techniques and x-ray diffraction. It was found that the size and quantity of sigma phase increased with time and temperature, in consonance with the nucleation and growth controlled by a diffusion process.

From the random distribution of sigma phase, and the absence of any observable layer on the OD of tubing, it appears that the sigma phase formation was not associated with sodium interaction (e.g., significant decarburization). This finding can further be substantiated by two observations:

1) Microstructural similarity of the specimens tested in sodium and helium environments

2) The relatively minute amount of sigma particles detected in the annealed tubing tested in sodium at a similar temperature and time.

Under the conditions of cold-worked alloys, temperature, and time in the stress-rupture tests conducted in this work, the formation of sigma phase in the tubing is predominantly due to the presence of cold work and high-temperature creep deformation of the metastable alloys.[27-29]

It is interesting to note the regions adjacent to a large sigma particle. The grain boundaries appear very diffuse, and the carbides appear to have been depleted (Figure 19c). This observation is attributed to the diffusion of chromium atoms away from carbides ($M_{23}C_6$) for the formation and growth of sigma particles, leaving the grain boundaries relatively depleted of carbides and chromium. The phase change and depletion of grain boundary carbides is significant because:

1) Thermodynamic instability might enhance creep rate, due to the increased diffusion

2) The depleted region could offer less resistance to dislocation movement, lowering the creep resistance of the material.

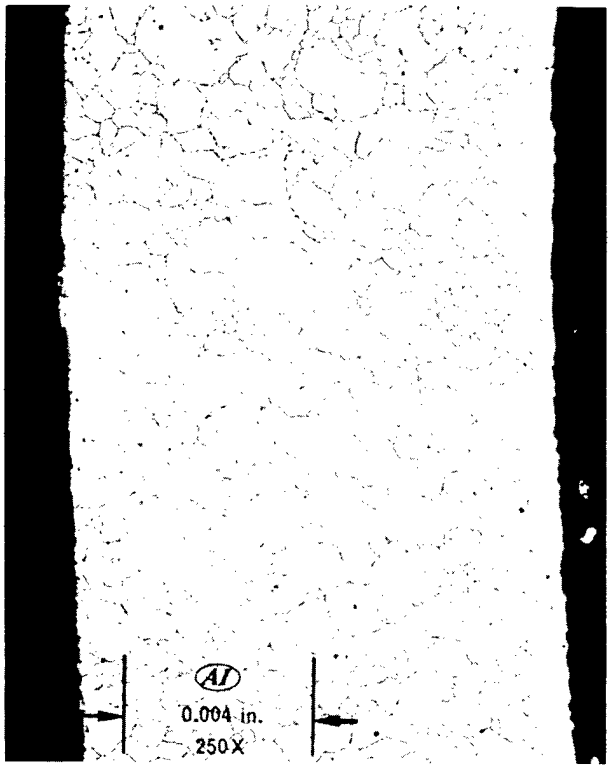

Etchant: Marble's Solution 8218-8-1

a. Tested in 1200° F Sodium for 3450 hr Without Stress

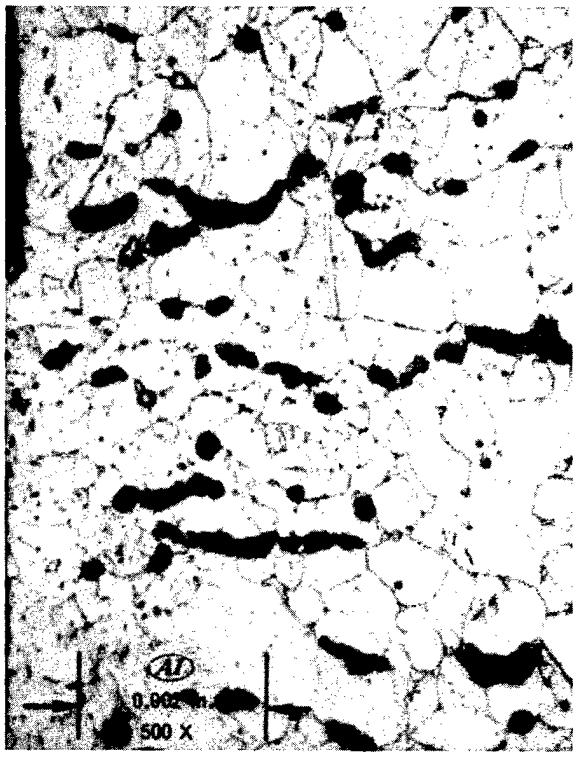

Etchant: Marble's Solution 8002-1-9

b. Tested in 1400° F Sodium for 850 hr (σ = 6800 psi, t_r = 813 hr, ϵ = 6%)

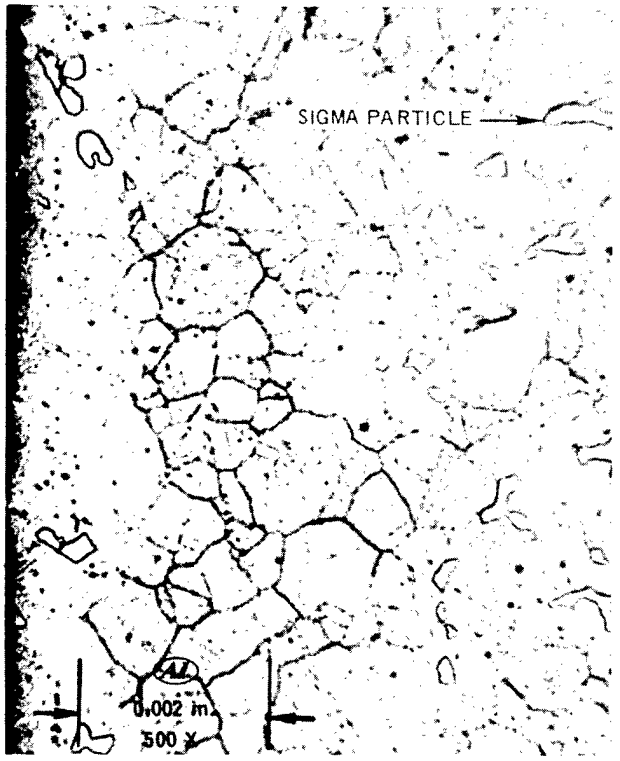

Etchant: Marble's Solution 8218-7-2

c. Tested in 1400° F Sodium for 3400 hr Without Stress (Note areas adjacent to sigma particles relatively depleted of carbides)

Figure 19. Effects of Temperature and Time on Sigma-Phase Formation and Growth in 10 to 15% Cold-Worked Type 304 Stainless Steel

The zones could act as sites for crack nucleation, because of their inherent low strength. This may be why cold-worked Type 316 stainless steel has significantly higher long-term rupture strength than the cold-worked Type 304 stainless steel tested at 1400°F.

D. INTERCRYSTALLINE FRACTURE

Metallographic examination of the ruptured Types 304 and 316 stainless steel tubing, stress-rupture tested in 1400 and 1200°F sodium, revealed the following:

1) All specimens exhibited intergranular failure.

2) All cold-worked samples showed extensive grain-boundary fissuring and little grain deformation. Those specimens tested in 1400°F sodium contained predominantly r-type grain boundary voids; specimens tested in 1200°F sodium contained a mixture of r-type and w-type grain-boundary voids. Grain-boundary fissuring was more extensive in specimens tested at 1400°F than in those tested at 1200°F. Most voids were associated with sigma particles or carbides; some voids were associated with triple points.

3) All annealed specimens showed few grain-boundary fissures, but some grain deformation, particularly at fracture areas.

Review of the mechanisms of fracture under high-temperature creep conditions ($T/T_m > 0.3$) indicates that, at low strain rates, fracture results from the formation and linkage of small voids on grain boundaries. McLean[30] has shown that creep of polycrystalline metals occurs by dislocation migration in the grains, resulting in slip and subgrain tilting, as well as by grain-boundary shearing. From the findings that the activation energy and creep law hold for grain-boundary shear, Dorn[31] suggested that grain-boundary shearing can be attributed to localized crystallographic mechanisms of deformation in the vicinity of the grain boundaries. As a result, the appearance of the grain-boundary voids in the tested specimens is dependent upon the material properties in the grain matrix.

For a temperature range of T/T_m between 0.40 to 0.55 (1000 to 1400°F, for both austenitic stainless steels), and at low strain rates, the grain-boundary

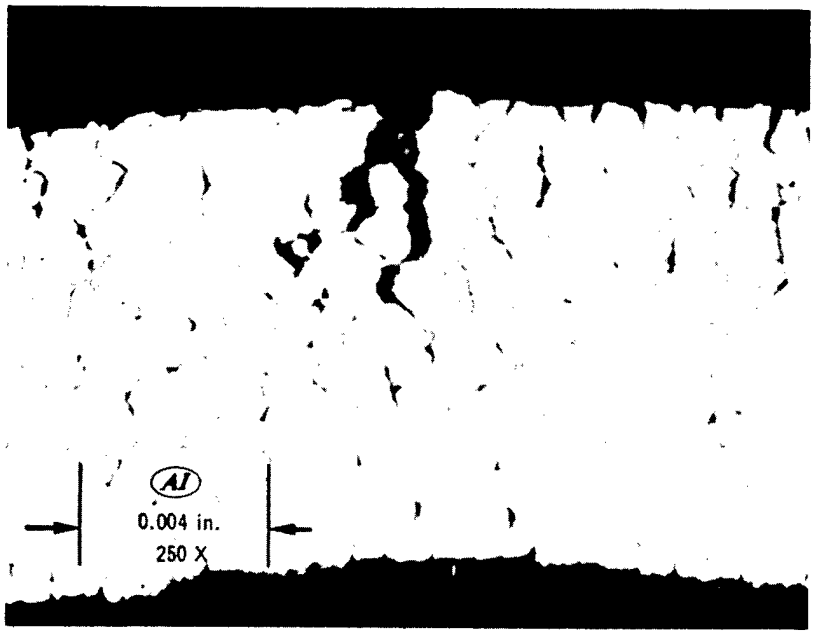

a. Annealed (σ = 7200 psi, t_r = 2120 hr, ϵ = 6%)

Etchant: Marble's Solution

8081-1-1

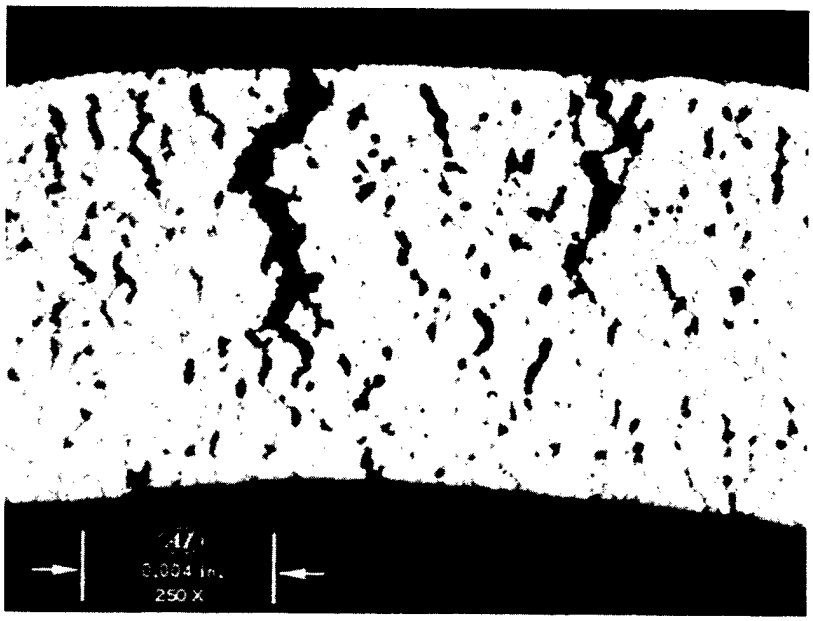

b. 10 to 15% Cold Work (σ = 6800 psi, t_r = 813 hr, ϵ = 6%)

Etchant: Marble's Solution

8002-1-5

Figure 20. Effect of Cold Work on Microstructure and Void Density of Type 304 Stainless Steel Stress-Rupture Tested in 1400° F Sodium

voids observed are nucleated by grain-boundary sliding, which generates high stress concentration at precipitates, at grain corners, or at ledges on the grain boundaries. This is readily realized if Stroh's equation is applied:[32]

$$\sigma_s = \left(\frac{12\mu\gamma_s}{\pi L}\right)^{1/2} \qquad \ldots(7)$$

where

σ_s = applied shear stress
L = length of sliding boundary between obstacles
μ = shear modulus
γ_s = surface energy at the interface.

As can be seen in the photomicrographs of 10 to 15% cold-worked Types 304 and 316 stainless steel, grain-boundary voids are associated with carbide and sigma particles on the grain boundaries, with few at the triple points. While voids at the triple points are probably nucleated according to Zener's mechanism,[33] voids found adjacent to carbides or sigma particles are nucleated in accordance with Stroh's intercrystalline fracture mechanism,[32] due to the reduction of the surface energy at the matrix-particle interface (for an incoherent interface). Applying a similar equation, Weaver,[34] and Kramer et al.,[17] substantiated the role of precipitates, mainly carbides, on grain boundaries of stainless steel in nucleating intergranular fissures.

The void density and size increased with the time and temperature of test. This behavior is attributable to vacancy migration (a diffusion-controlled process) to the void for growth (coalescence) while the sliding process is still in progress.[35] As a result, the final rupture appears to be caused by the growth and linkage of the existing voids on the grain boundaries. The rate of propagation of voids determined the life of the material and the location of the fracture.

The cold-worked material exhibited extensive grain-boundary fissuring, with little grain deformation. On the other hand, annealed specimens show some grain deformation, particularly at rupture areas, and little grain-boundary voids (Figure 20). The difference between cold-worked and annealed austenitic stainless steel is attributed to the effects of grain hardening which reduced the deformability of the cold-worked material, and to weakening of the grain boundary by prior cold work.[13]

Although it is an obvious direct cause of intergranular fracture, grain-boundary sliding does not always lead to fracture. Servi and Grant[36] have shown that pure aluminum resisted intergranular fracture and remained very ductile at all temperatures up to the melting point, even though copious grain-boundary sliding occurred. High stress concentrations at grain corners, due to grain-boundary sliding, occurred; but they were relaxed by plastic deformation in the grain at the end of the sliding boundary, giving rise to a plastic fold. This type of stress concentration can also be relaxed or dispersed by grain-boundary migration.[37] Such plastic deformation and grain-boundary migration are found in specimens of the annealed Types 316 and 304 stainless steel (Figures 5 and 10). Extensive grain-boundary-zone shear and grain-boundary migration are also evident. Hardening of grains, to improve creep resistance, is likely to promote intercrystalline fracture when tested at high temperatures, as was observed in this work. Similar observations have also been reported by Glen,[38] on low carbon steel; and by Irvine et al.,[39] and Young et al.,[40] on niobium-bearing austenitic stainless steels.

V. CONCLUSIONS

Studies on the stress-rupture behavior of one heat of Type 304 stainless steel and one heat of Type 316 stainless steel in high-purity sodium ($O_2 \sim 10$ ppm) and helium (99.99% pure) revealed the following:

1) No significant degradation of mechanical properties was found in a high-purity sodium environment, for testing times up to 3000 hr at 1200°F and 1000 hr at 1400°F.

2) The internal stresses due to 10 to 15% cold work did not induce intercrystalline penetration by liquid sodium.

3) Use of 10 to 15% cold work reduced long-term stress-rupture properties to below the properties for annealed material for both Type 304 and Type 316 stainless steel at 1200 and 1400°F. The 10 to 15% cold work also decreased the activation energy for creep; the effect was more pronounced for Type 304 stainless steel.

4) Cold work enhanced precipitation within grains and weakened the grain boundary, promoting extensive grain-boundary void formation, due to grain-boundary sliding.

5) The formation of sigma phase in tested specimens was attributable to the presence of cold work and deformation during the stress-rupture test at high temperature.

6) Above 1200°F, 10 to 15% cold-worked Type 316 stainless steel exhibited significantly higher long-term rupture strength than cold-worked Type 304 stainless steel, and comparable ductility (diametral strain). At 1000°F, cold-worked Type 304 stainless steel had a higher rupture strength.

Because of the interim nature of this report, many features of the mechanical behavior of austenitic stainless steels in high-purity sodium remain to be investigated. Studies will be continued, to gain a better statistical confidence in the data for the temperature range of 900 to 1400°F. Stress-rupture data will be obtained for rupture times to 10,000 hr; the effect of the state of stress will be explored; and a quantitative relationship between stress-rupture behavior and the degree of cold work will be developed.

REFERENCES

1. V. W. Eldred, "Interactions Between Solid and Liquid Metals and Alloys," Atomic Energy Research Establishment Report X/R 1806 (1953)

2. C. S. Smith, "Measurement of Interfacial Tensions," Trans. AIME, 175 (1948) pp 15-51

3. W. T. Lee, "Biaxial Stress-Rupture Properties of Austenitic Stainless Steels in Zirconium-Gettered Sodium," NAA-SR-12353 (October 1, 1967)

4. J. W. Martin and G. E. Smith, "A Preliminary Study of the Fatigue of Metals in Liquid Metal Environments," Metallurgia 54 (1956) pp 227-232

5. N. J. Grant and A. W. Mullendore, Deformation and Fracture at Elevated Temperature (MIT Press, Cambridge, Mass., 1965) p 198

6. R. C. Andrews et al., "Effect of High Temperature Sodium on Austenitic and Ferritic Steels," MSAR 67-216 (December 1967)

7. W. Rostoker, J. M. McGaughey, and H. Markus, Embrittlement by Liquid Metals (Reinhold Publishing Corp., New York, 1960) p 14

8. ASTM Standards, Part 31 (May 1967) p 453

9. R. J. Roark, Formula for Stress and Strain (McGraw-Hill Book Co., New York, 1954) p 268

10. H. K. Richardson and R. McDowell, "Elevated Temperature Stress Rupture Properties of M316, FV 548, and Nimonic PE 16 P. F. R. -Type Tube," TRG Report 1482(c) (1967)

11. T. M. Krebs and N. Soltys, Joint International Conference on Creep, P34, (1963) pp 1-12

12. "Properties and Selection," Metals Handbook, Vol 1, ASM (1967) p 473

13. W. Siegfried, "Investigation Into the Development of Intercrystalline Fracture in Various Steels Under Triaxial Stress," Creep and Fracture of Metals at High Temperature, Proceeding of a Symposium held at the National Physical Laboratory (1954) p 336

14. R. Lagneborg, "Deviations From Linearity in Creep-Rupture Curves," Metal Science Journal, 1 (1967) p 172

15. N. J. Grant and A. G. Bucklin, "Creep-Rupture and Recrystallization of Monel, 700 to 1700° F," ASM Trans., 45 (1953) p 151

16. F. C. Monkman, P.E. Price, and N. J. Grant, "The Effect of Composition and Structure on the Creep-Rupture Properties of 18-8 Stainless Steel," ASM Trans., 48 (1956) p 418

17. D. Kramer et al., "Helium Embrittlement in Type 304 Stainless Steel," NAA-SR-12601 (December 5, 1967)

18. A. H. Cottrell, Dislocations and Plastic Flow in Crystals (Oxford Press, London, 1956) p 132

19. J. E. Dorn, P. R. Landon, J. L. Lytton, and L. A. Sheppard, "The Activation Energies for Creep of Polycrystalline Copper and Nickel," ASM Trans., 51 (1959) p 900

20. F. Garofalo, Fundamentals of Creep and Creep-Rupture in Metals (Macmillan Co., New York, 1966) p 83

21. J. T. Venard, "Stress-Rupture Properties of Type 304 Stainless Steel Tubing," ORNL-TM-535 (1963)

22. A. L. Titchener and M. B. Bever, "The Stored Energy of Cold Work," Progress in Metal Physics (1958)

23. W. A. Anderson and R. F. Mehl, "Recrystallization of Aluminum in Terms of the Rate of Nucleation and the Rate of Growth," Trans. AIME, 161 (1945) pp 140-167

24. M. Cook and T. L. Richards, "The Tensile-Shear Stress Ratio in Rolled Copper Alloys," Journal Institute of Metals, 14 (1947) pp 541-551

25. G. W. Wench et al., "Recrystallization of Tantalum," Trans. ASM, 44 (1952) p 596

26. Unpublished Notebook Data, Atomics International, Canoga Park, California (1968)

27. F. B. Cuff and N. J. Grant, "The Effect of Cold Work on the Creep-Rupture Properties of a Series of 18-8 Type Stainless Steels," J. of Iron & Steel Institute, 186 (1957) pp 188-197

28. G. F. Tisinai, J. K. Stanley, C. H. Samans, "Sigma Nucleation Times in Stainless Steels," J. of Metals Trans., AIME (1956) pp 600-604

29. J. Dulis, G. V. Smith, and E. G. Houston, "Creep and Rupture of Chromium-Nickel Austenitic Stainless Steels," ASM Trans. 45 (1953) pp 42-76

30. D. McLean, "Grain-Boundary Slip During Creep of Aluminum," J. Institute of Metals, 81 (1952-53) pp 293-300

31. J. E. Dorn, B. Fazen, and O. D. Sherby, "Some Observations on Grain Boundary Shearing During Creep," J.of Metals, Trans. AIME, 200 (1954) p 919

32. A. N. Stroh, "The Formation of Cracks as a Result of Plastic Flow," Proc. Roy Soc., 223 (A) (1954) p 404

33. C. Zener, Fracturing of Metals, Ed., G. Sachs (ASM, 1948)

34. C. W. Weaver, "Application of Stroh's Theory to Intercrystalline Creep Cracking," Acta Met., 8 (1960) p 343

35. C. W. Chen and E. S. Machlin, "On the Mechanism of Intercrystalline Cracking," Acta Met., 4 (1956) p 655

36. I. S. Servi and N. J. Grant, "Creep and Stress Rupture Behavior of Aluminum as a Function of Purity," AIME Trans., 191 (1951) p 909

37. R. C. Gifkins, Fracture, Ed., B. L. Averbach et al., (MIT Press, Cambridge, Mass., 1959) p 579

38. J. Glen, "Ductility in High Temperature Rupture Tests," J. of Iron & Steel Institute, 190 (1958) pp 30-39

39. K. J. Irvine et al., "The Effect of Heat Treatment and Microstructure on the High Temperature Ductility of 18% Cr - 12% Ni - 1% Nb Steels," J. of Iron & Steel Institute, 196 (1960) pp 166-179

40. R. N. Younger and R. G. Baker, "Heat-Affected Zone Cracking in Welded High-Temperature Austenitic Steels," J. of Iron & Steel Institute, 196 (1960) pp 188-194